APPLICATIONS OF MOLYBDENUM UTILIZED IN SENSING DEVICES

By

DEREK DAVIN BUSSAN

Bachelor of Arts in Chemistry

University of Iowa

Iowa City, IA

2004

Submitted to the Faculty of the
Graduate College of the
Oklahoma State University
in partial fulfillment of
the requirements for
the Degree of
MASTER OF SCIENCE
May, 2011

APPLICATIONS OF MOLYBDENUM UTILIZED IN

SENSING DEVICES

Thesis Approved:

Dr. Allen W. Apblett

Thesis Adviser

Dr. Nicholas F. Materer

Committee Member

Dr. Kenneth D. Berlin

Committee Member

Dr. Mark E. Payton

Dean of the Graduate College

.

ACKNOWLEDGMENTS

I wish to first express my sincere appreciation and gratefulness to God and Jesus Christ my lord and savior. Without them I know I would of never made it through this long journey. In this journey, called graduate school, there have been good times and bad times, and they have never let me down at any step along the way. I would next like to thank my parents Ron and Michele Bussan. My parents are the ones who taught me how to get through life, and they never stopped believing in me and have always wanted the best for me. I enjoyed when they first brought me down to Stillwater Oklahoma, and how they came to visit me in Stillwater at least twice a year. I would like to thank my sister Rachel Bussan and my niece Chelsea Bussan for an inspiration on life to think on other subject matter other then chemistry. I would also like to thank my fiancé Kimberly Savaglio for being with me every step of the way in my graduate studies. I would also like to thank Kimberly for not giving up on me, and for the times that we had in and out of Stillwater, Oklahoma.

I would like to thank my advisor Dr. Allen W. Apblett for giving me an opportunity to work in his lab and for the funding he provided while I was on a research assistantship. I would like to thank Dr. Nicholas F. Materer for allowing me to use his lab to get my research done. I would also like to thank everyone in the chemistry office namely Bob Kirkley, Karen Munday, and Cheryl Malone, for without the office staff, things would flow much harder in the chemistry office. I would like to thank my mentor Dr. Kevin N. Barber for he mentored me through my first two years of graduate school. I would also like to thank Daniel Hoel, for all the work he has done helping me along the way so that I could graduate. I would also like to thank the class that I came in with “2008” and all my lab mates. And lastly Dr. Berlin for showing me the ropes.

TABLE OF CONTENTS

Chapter Page

LIST OF TABLES

Table Page

LIST OF FIGURES

Figure Page

Figure Page

LIST OF REACTIONS

LIST OF SCHEMES

CHAPTER I

Introduction

Background

The need for novel ways to look for explosives and terrorist based explosives is going to continue well into the 21st century. Explosions need not be limited to airports, train stations, buses, and attacks on U.S and N.A.T.O troops, but explosions could just as well occur in a laboratory setting. This thesis will help explain the need for a highly sensitive material that can detect these types of explosives.

Explosives-"are solid or liquid substances, individually or mixed with one another, which are in a metastable state, and are capable, for this reason, of undergoing a rapid chemical reaction without the participation of external reactants such as atmospheric oxygen." An explosive reaction can be initiated by mechanical means (impact, impact sensitivity; friction, friction sensitivity), by the action of heat (sparks, open flame, red-hot or white-hot objects) or by detonating shock (blasting cap) with or without a booster charge). The resistance of the metastable state to heat is known as stability. The ease with which the chemical reaction can be initiated is known as sensitivity.

The reaction products are predominantly gaseous (fumes). The propagation rate from the initiation site outwards through the explosive material may be much slower then the velocity of

sound (→ deflagration; → gunpowder) or can be supersonic (→ detonation). Explosives are solid, liquid or gelatinous substances or mixtures of individual substances, which have been manufactured for blasting or propulsion purposes. For their effectiveness → strength; → burning rate; → brisance.

Materials which are not intended to be used for blasting or shooting may also be explosive. They include, for example, organic peroxide catalysts, gas-liberating agents employed in the modern manufacture of plastic materials and plastic foams, certain kinds of insecticides, etc. The explosive potential of many substances is unknown; thus, for instance, this is the case, if they are capable of undergoing an extremely exothermic polymerization or rearrangement reaction.[1]

Since the dawn of the Oklahoma City bombing when Timothy McVeigh drove a Ryder truck on April 19, 1995, Oklahoma is a prime area to be conducting research on novel ways of finding terrorist explosives. Although McVeigh used ammonium nitrate and nitromethane, a similar catastrophe could occur, using peroxide based explosives. On December 21, 2001, passengers on flight 63 complained of a smoke smell, which was later found to be Richard Reid a passenger who was trying to light up a bomb composed of pentaerythritol tetranitrate (PETN), plastic chemicals to gel and mold the explosives, and triacetone triperoxide (TATP).[2] Fortunately there was no catastrophe from this incident since the passengers and crew subdued Reid but if Reid was successful, the "What ifs" could have been horrific.

This thesis will show an effective and quick method of detecting peroxide based explosives (PBEs) that is cost effective and, in one method of detecting the PBE's, it is also environmentally friendly.

Types of Peroxide based Explosives:

Triacetone triperoxide(TATP):

Triacetone triperoxide ($C_6H_{12}O_4$) is a highly effective explosive that can be made at the home with a few simple ingredients mainly hydrogen peroxide, acetone, and sulfuric acid used as a catalyst.[3] The recipe is

readily available on the internet. If 27 or 30% hydrogen peroxide can be found, then it will produce higher yields when used. However, a change in the percentage will mean a change in the ratio or amount used. The ratio involved uses 3% hydrogen peroxide, because of its availability. The 3% hydrogen peroxide can be easily bought at any drug store, pharmacy, or local convenient store. It can be found in the medical aisle at Jewel.[3] This internet recipe not only gives you the percentage of hydrogen peroxide to use but also specifies where to go get the necessary ingredients and the synthesis process for making TATP. The acid catalyzed synthesis was first described in 1959 by Millas,[4] who slowly added acetone (0.2 mol) at 0 °C to a cold mixture of hydrogen peroxide (50%, 0.2 mol) and sulfuric acid, kept the mixture at 0 °C for 3 h, and then extracted it with pentane. TATP has power close to that of TNT (a 10 g sample gave 250 cm^3 expansion in the Trauzl test as compared to 300 cm^3 for TNT).[5] TATP can be used as an explosive and a main charge for detonation, and thus is a key ingredient in many improvised bombs. TATP and other cyclic peroxides have attracted increasing interest because these readily available compounds are extensively used by terrorist organizations worldwide for manufacturing of improvised explosive devices. The physical properties of these cyclic peroxides are of particular interest because the lack of any nitrogen functionality in the molecule makes their detection and identification by standard explosive

detectors an extremely difficult task.[6,7] TATP gets its instability from having 3 oxygen-oxygen bonds in its molecule.

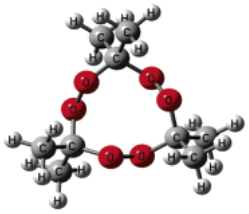

1-D_3
O-O bonds
lengths: 1.462

Figure 1.1. One of the conformers of TATP[8]

Figure 1.1 shows one of the possible conformers of TATP. This conformer shows TATP in its most stable state. The procedure for making TATP is given in a book titled "Chemical Demonstrations" by Bassam Z. Shakhashiri.[9] The procedure for synthesizing TATP according to Shakhashiri is as follows: Wear gloves while preparing the peroxyacetone. Add 4 ml of acetone and 4 ml of 30% hydrogen peroxide to a 150-mm test tube. Then add 4 drops of concentrated hydrochloric acid to the mixture. In 10-20 minutes a white solid should begin to separate from the solution. If no change is observed, warm the test tube in a water bath at 40 ^{o}C to initiate the reaction. Allow the reaction to continue for 2 hours. Swirl the slurry and filter it. Rinse the solid remaining in the test tube onto the filter paper with small portions of distilled water. Open the filter paper on a watch glass and allow the peroxyacetone solid to dry for at least 2 hours.[9] Shakhashiri notes to "not ignite the peroxyacetone from a distance of less than 1m. Do not drop or jar the solid, since it is shock sensitive. Use all the solid prepared; do not store it."[9] TATP is extremely flammable and hazardous and with the above recipe, TATP can easily be prepared.

Hexamethylene triperoxide diamine (HMTD):

Hexamethylene triperoxide diamine ($C_6H_{12}N_2O_6$) is another peroxide based explosive like TATP that can be made by the general public with everyday materials. HMTD was originally discovered in Germany by Legler[10] in 1885. The structure of HMTD is shown in Figure 1.2.

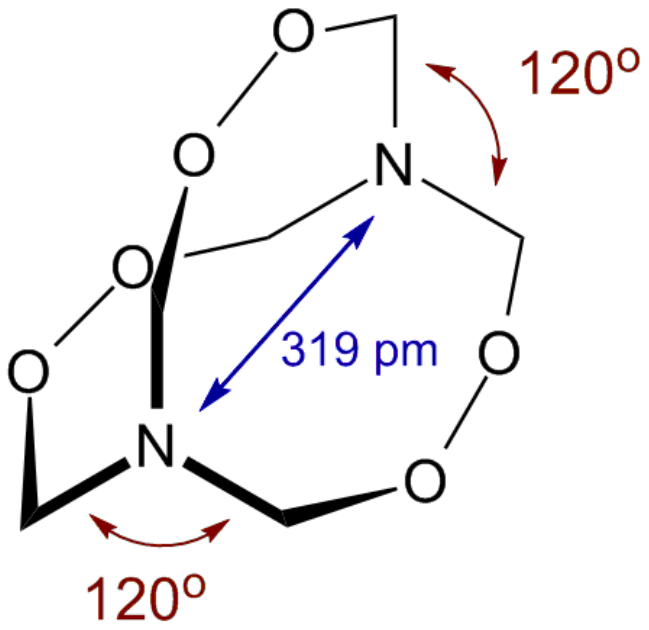

Figure 1.2. The structure of HMTD[11,12]

The preparation of HMTD is given in Tenney L. Davis book titled "The Chemistry of Powder and Explosives."[13] The chemical reaction is as follows:[13]

$$\mathbf{C_6H_{12}N_4 + 3H_2O_2 \rightarrow C_6H_{12}N_2O_6 + 2NH_4}$$

Preparation of Hexamethylenetriperoxidediamine. Fourteen grams of hexamethlenetetramine is dissolved in 45 grams of 30% hydrogen peroxide solution which is stirred mechanically in a beaker standing in a freezing mixture of cracked ice with water and a little salt. To the solution 21 grams of powdered citric acid is added slowly in small portions at a time while the stirring is continued and the temperature of the mixture is kept at 0 ^{o}C or below. After all the citric acid has dissolved, the mixture is stirred for 3 hours longer while its temperature is kept at 0 ^{o}C. Cooling is then discontinued, the mixture is allowed to stand for 2 hours at room temperature, and the white crystalline product is filtered off,

washed thoroughly with water, and rinsed with alcohol in order that it may dry out more quickly at ordinary temperatures.[13] Davis does comment that this is the only organic peroxide seriously considered as an explosive, but never was practical due to being too chemically reactive and unstable.[13]

Introduction to Molybdenum Bronzes:

The term bronze was originally coined for Na_xWO_3 compounds by Wohler in 1825.[14] The term bronze is applied to a variety of transition metal oxides, and they are usually ternary compounds with the formula $A_xM_zO_y$. These compounds usually have an intense color, metallic luster, metallic or semiconducting properties, and are resistant to attack by nonoxidizing acids.[15] Ternary bronzes have been prepared in which M is Ti, V, Mn, Nb, Ta, Mo, W, or Re, and A is H, NH_4^+, or an alkali, alkaline earth, rare earth, group 11, group 12, or other metal ion.[15] The bronzes discussed in this thesis will be of the form from molybdenum.

Molybdenum bronzes have been in the scientific literature as far back as 1895 when Stavenhagen and Engels[16] prepared sodium molybdenum bronze by electrolytic reduction of fused sodium molybdate. Wold et al.[17] prepared sodium and molybdenum bronze crystals by electrolytic reduction, of sodium and potassium molybdenum bronze single crystals.[17] In 1895 Charles Hatch Ehrenfeld noticed that when slowly heated in air molybdenum oxides change from brown and blue oxides until the oxides reach their most stable form which is molybdenum trioxide.[18] In 1963 Wold, et al. found that the successful preparation of alkali metal molybdenum bronzes is dependent upon both the reduction temperature and the molar ratio of alkali metal molybdate to molybdenum(VI) oxide.[17]

Molybdenum trioxide possesses a unique layered structure consisting of double chains of edge-sharing MoO_6 octahedra linked through vertices to form infinite channeled layers held together by van der Waals forces.[19] Due to this layered structure of MoO_3, MoO_3 becomes the perfect candidate to intercalate the various layers of its structure with hydrogen atoms leading up to the definition of a hydrogen-molybdenum bronze. Figure 1.3 shows a hydrogen molybdenum bronze phase.[20]

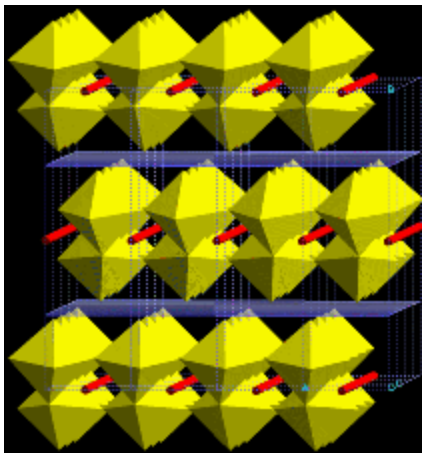

Figure 1.3. A structure of molybdenum hydrogen bronze[20]

Figure 1.3 shows a hydgrogen molybdenum bronze phase formed by the intercalation of atomic hydrogen. The channels within the octahedral layers are marked by sticks.[20]

Glemser et al. synthesized four solid phases of H_xMoO_3 $0<x<2.0$.[21,22,23] The phases of H_xMoO_3 were then later characterized by J.J. Birtill and P.G. Dickens.[24] Birtill and Dickens based therir analysis on reducing power, thermogravimetry, and powder X-ray diffraction. The following Table 1.1 shows the results of Birtill and Dickens findings.[24]

Table 1.1

Pure Phases H_xMoO_3

Code	Formula	Reducing Power	Thermogravimetry	Description
S39	$H_{0.28}MoO_3$	0.28±0.01	_	Dark blue. Orthorhombic
S25	$H_{0.34}MoO_3$	0.34± 0.02	0.35± 0.02	Dark blue. Orthorhombic
R1	$H_{0.34}MoO_3$	0.34± 0.01	0.35±0.02	Dark blue. Orthorhombic
S35	$D_{0.3666}MoO_3$	0.366±0.003	_	Dark blue. Orthorhombic
S13	$H_{0.88}MoO_3$	_	0.88±0.03	Dark blue. Monoclinic
S28	$H_{0.093}MoO_3$	0.932±0.003	0.93	Dark blue. Monoclinic
S40	$H_{1.55}MoO_3$	1.55±0.01	_	Deep red. Monoclinic
R9*	$H_{1.68}MoO_3$	1.68±0.01	1.68±0.01	Deep red. Monoclinic
R11*	$D_{1.7}MoO_3$	_	1.7	Deep red. Monoclinic
R22*	$H_{1.72}MoO_3$	1.72±0.01	_	As S40, but very slight trace(x-ray) of $H_{2.0}MoO_3$
R19	$H_{2.0}MoO_3$	1.99±0.02	_	Dark green. Monoclinic
R24	'$D_{2.0}MoO_3$'	_	_	Dark green. Monoclinic
R22		1.93±0.02		As R19 but contained red monoclinc (x-ray)

Figures in parentheses indicate no. of analytical determinations.

***Produced by thermal dehydrogenation of $H_{2.0}MoO_3$ in 110 ^oC in Vacuo.**

Code 'S' indicates production by 'equilibration' in sealed tube with H_2O. Code 'R' indicated production by Zn/HCl reduction.

According to the Table 1.1 most hydrogen molybdenum bronzes H_xMoO_3 fall into two types of crystal systems that is either orthorhombic or monoclinic. Table 1.2 is a chart of the two types of crystals systems from Anthony R. West book on "Solid State Chemistry and its Applications."[25]

Table 1.2

Two types of crystal systems[25]

Crystal System	Unit cell shape	Essential symmetry	Space lattices
Orthorhombic	$a \neq b \neq c$, $\alpha=\beta=\gamma=90^o$	Three twofold axes or mirror planes	P, F, I, A(B or C)
Monoclinic	$a \neq b \neq c$, $\alpha=\gamma=90^o$, $\beta \neq 90^o$	One twofold axis or mirror plane	P,C

The "P" stands for primitive unit cell and has a point at each corner. The "I" stands for body-centered unit cell. And has a lattice point at each corner and one at the center of the cell. The "F" stands for face-centered unit cell. And has a lattice point at each corner and one in the center of the face. The"A", "B", and "C" stand for face-centered unit cell. And has a lattice point at each corner, and one in the centers of one pair of opposite faces (e.g., an A-centered cell has lattice points in the centers of the *bc* faces).[26]

CHAPTER II

Current Methods for Detecting Peroxide Based Explosives and H_2O_2

The first analytical methods for determining TATP and HMTD published were intended for the identification of synthesized products or suspicious materials.[27] Since terrorist did not have to worry about setting off any X-ray alarms at airports, due to these compounds not containing any heavy metals. TATP is one peroxide based explosives that can decompose into acetone, ozone[28] and hydrogen peroxide due to its high volatility. Possible methods of detection utilize the fact that acetone and hydrogen peroxide vapor are given off. HMTD has a low vapor pressure and needs other methods of detection. Since TATP and HMTD compounds are sensitive to shock, friction, and impact, extreme care must also be used to prevent accidents to the scientist analyzing these compounds.[27]

Melting Point Analysis:

One obvious point of detecting TATP and HMTD would be a melting point analysis. The melting points of TATP and HMTD are known to be 96 ^{o}C for TATP and 148 ^{o}C for HMTD, respectively.[29] Both TATP and HMTD are both highly explosive, and these compounds should not be heated to melting without taking great precautions. In the case with HMTD, the compound decomposes rapidly when it hit its melting point and also turns yellow.[30] Melting point analysis is therefore not very feasible due to the high explosive nature of the compounds involved.

Infrared, Raman, and NMR Spectroscopy:

In 1988 Suzle, et al studied the Infrared, Raman, and NMR spectra of HMTD.[30] They recorded the IR spectra with a Perkin-Elmer model 225. HMTD is practically insoluble in non-polar solvents (CS_2, CCl_4, C_6H_6, and C_6H_{12}), and only very slightly soluble in dimethyl sulfoxide (DMSO) or N,N-dimethlyformamide (DMF) and therefore no IR could be prepared in solution.[30] Consequently the HMTD sample was prepared using pellets in KBr and polyethylene and as a Nujol mull between CsI plates. Figure 2.1 shows the IR spectrum of HMTD from Suzle, et al.[30]

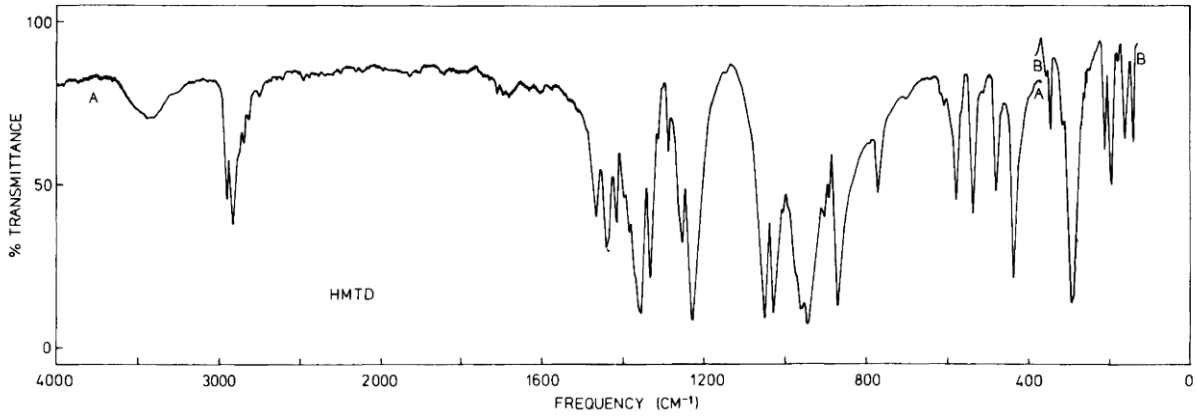

Figure 2.1. IR spectra of hexamethylene triperoxide diamine[30]

Suzle et al. also took a Raman and NMR spectra of HMDT which is shown in Figures 2.2 and 2.3.

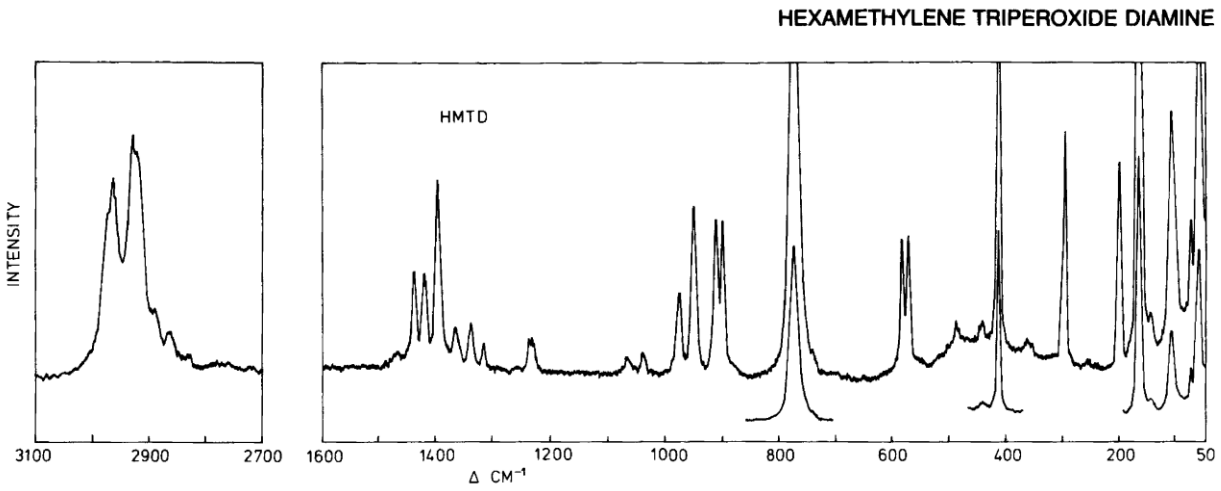

Figure 2.2. Raman spectra of HMTD[30]

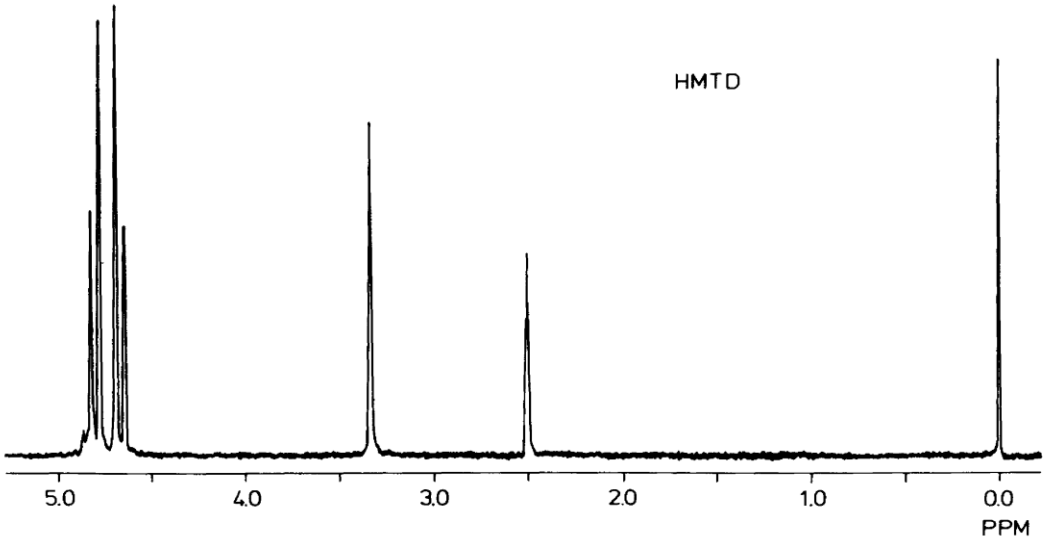

Figure 2.3. NMR spectra of HMDT[30]

In the IR spectra one can note at 1680 cm^{-1} must be attributed to a carbonyl moiety, that's possibly from the aldehyde groups that are formed by the cleavage of one of the O-O bonds. The proton spectrum above contains proton peaks at 298 k at 4.644, 4.689, 4.777, and 4.823 ppm. While if the temperature is raised to 323 K the peaks are found at 4.624, 4.691, 4.768, and 4.835 ppm. The author explained the quarter around 2.5 ppm, and a broad line at 3.336 ppm were due to impurities of DMSO-d_5 and water. The author then claims with the above information they were able to confirm the D3 symmetry of HMTD. One note on the above experiment is when the author did Raman at 150 mW there was an explosion.[30]

Luminescence methods:

Analysis tests based on changes in color, fluorescence changes, or chemiluminescence can provide quick and reliable results for a variety of targets. Trogler et al. developed a method for detecting peroxide vapors down to the ppb[31]. Trogler et al. synthesized a polymer called PolyF-1 (3',6'-bis(pinacolatoboron)fluoran[31]. The author then used thin-films of PolyF-1 drop-cast onto aWhatman2 porous sampling substrate to increase the surface area for polymer-analyte interactions. The reaction of PolyF-1 with H_2O_2 is shown in Scheme 2.1.

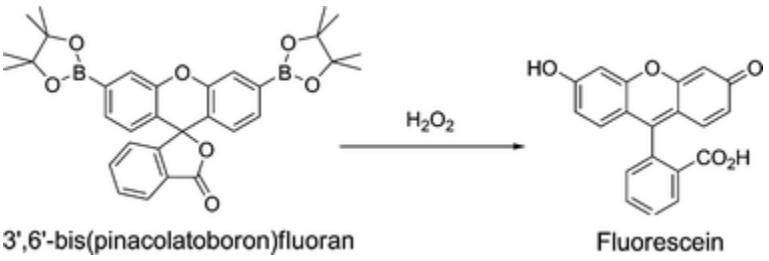

Scheme 2.1. PolyF-1 reacting with H_2O_2[31]

When exposed to H_2O_2 vapors the following colorimetric change can be seen, which is demonstrated in Figure 2.4.

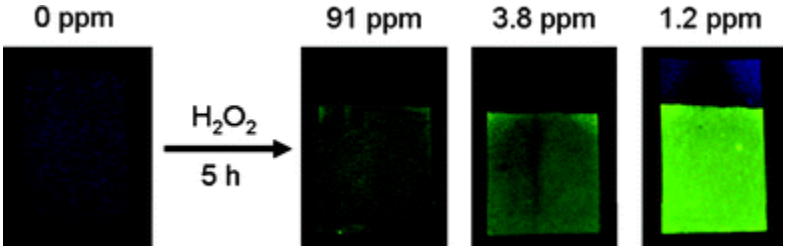

Figure 2.4. Images of the fluorescence response of 10 µg cm^{-2} PolyF-1 to various concentrations of H_2O_2 vapor over a 5 h period. An increase in fluorescence intensity is observed at lower concentrations of H_2O_2 providing a highly sensitive senor response[31]

Observing Figure 2.4 the author has demonstrated a low detection limit for detecting H_2O_2 vapors that could possibly used in a test strip format.

Hong et al. have recently developed a high-performance liquid chromatography method in which some higher peroxides used in the polymer industries (cumene hydroperoxide, *t*-butylhydroperoxide, di-*t*-butyl peroxide, *t*-butyl perbenzoate and t-butylcumyl peroxide) are decomposed by UV light in an on-line photochemical reactor[32]. Hong et al. stated "After HPLC separation a post-column photoreactor converts various organic peroxides to H_2O_2 and hydroperoxides, which then react with the derivatization agents p-hydroxyphenylacetic acid (PHPAA) and horseradish peroxidase (HRP) to form the fluorescent PHPAA dimer[32]".

CHAPTER III

Butanol Bronze

Experimental Section:

Purpose:

Chapter three describes a butanol bronze based-ink that is synthesized so for the applicablication for detecting, and neutralizing peroxides. From Apblett, et. al the solid molybdenum blue reacts rapidly with solutions of hydrogen peroxide and organic peroxides to yield MoO_3 and water or alcohols.[6] The following reactions shows how the hydrogen bronze reacts with hydrogen peroxide, or an organic peroxide.[6]

$$\mathbf{2Mo_2O_5(OH) + H_2O_2 \rightarrow 4MoO_3 + 2H_2O}$$

Reaction 3.1. Reaction of hydrogen blue bronze with H_20_2[6]

$$\mathbf{2Mo_2O_5(OH) + ROOH \rightarrow 4MoO_3 + H_2O + ROH}$$

Reaction 3.2. Reaction of hydrogen blue bronze with ROOH[6]

Scheme 3.1 shows how the molybdenum blue neutralizes an explosive. This scheme the molybdenum blue is neutralizing trinitrotoluene (TNT). The scheme depicts protons and electrons being shuttled from the molybdenum blue toward the very reactive TNT and rendering it into a nonviable explosive.

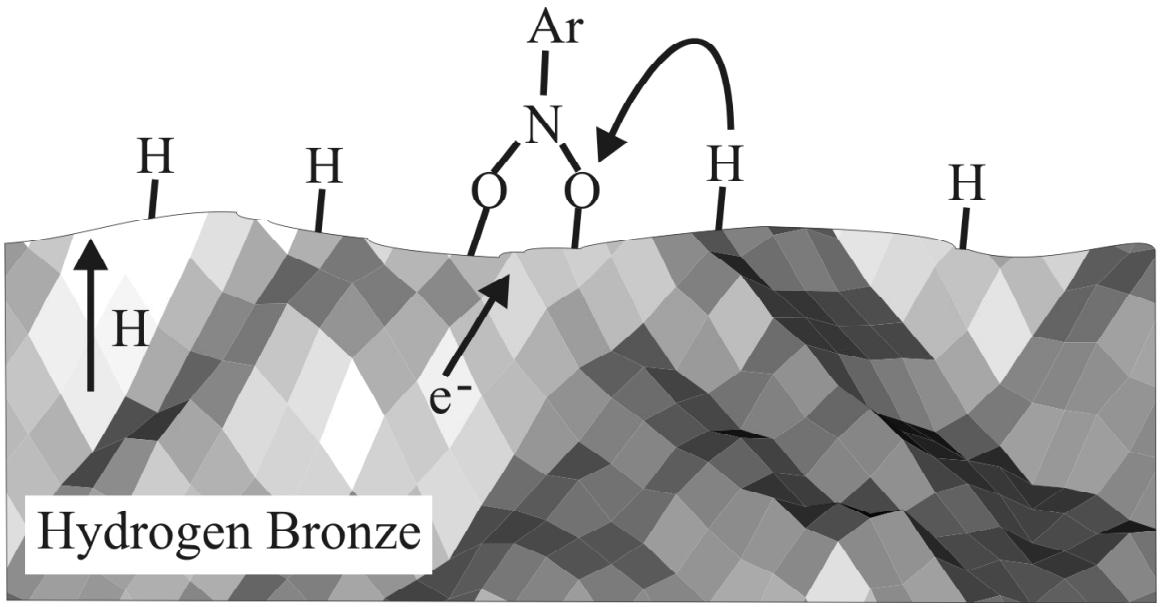

Scheme 3.1. Hydrogen bronze neutralizing trinitrotoluene[6]

Experimental:

All chemicals were reagent grade (ACS reagent grade) and were utilized without further purification. Ultra Violet spectrum were characterized using a [Carey 50]. The camera work was done using Dr. Materer's lab camera and then utilizing the program ImageJ from the National Institute of Health to analyze the kinetic data. From the ImageJ website, this is what ImageJ is capable of doing:

"**Runs Everywhere:**

> ImageJ is written in Java, which allows it to run on Linux, Mac OS X and Windows in both 32-bit and 64-bit modes.

Open Source:

ImageJ and its Java source code are freely available and in the public domain. No license is required.

User Community:

ImageJ has a large and knowledgeable worldwide user community. More than 1700 users and developers subscribe to the ImageJ mailing list.

Macros:

Automate tasks and create custom tools using macros. Generate macro code using thecommand recorder and debug it using the macro debugger. More than 300 macros are available on the ImageJ Web site.

Plugins:

Extend ImageJ by developing plugins using ImageJ's built in text editor and Java compiler. More than 500 plugins are available.

Toolkit:

Use ImageJ as a image processing toolkit (class library) to develop applets, servlets or applications.

Speed:

ImageJ is the world's fastest pure Java image processing program. It can filter a 2048x2048 image in 0.1 seconds (*). That's 40 million pixels per second!

Data Types:

8-bit grayscale or indexed color, 16-bit unsigned integer, 32-bit floating-point and RGB color.

File Formats:

Open and save all supported data types as TIFF (uncompressed) or as raw data. Open and save GIF, JPEG, BMP, PNG, PGM, FITS and ASCII. Open DICOM. Open TIFFs, GIFs, JPEGs, DICOMs and raw data using a URL. Open and save many other formats using plugins.

Image display:

Tools are provided for zooming (1:32 to 32:1) and scrolling images. All analysis and processing functions work at any magnification factor.

Selections:

Create rectangular, elliptical or irregular area selections. Create line and point selections. Edit selectoins and automatically create them using the wand tool. Draw, fill, clear, filter or measure selections. Save selections and transer them to other images.

Image Enhancement:

Supports smoothing, sharpening, edge detection, median filtering and thresholding on both 8-bit grayscale and RGB color images. Interactively adjust brightness and contrast of 8, 16 and 32-bit images.

Geometric Operations:

Crop, scale, resize and rotate. Flip vertically or horizontally.

Analysis:

Measure area, mean, standard deviation, min and max of selection or entire image. Measure lengths and angles. Use real world measurement units such as millimeters. Calibrate using density standards. Generate histograms and profile plots.

Editing:

Cut, copy or paste images or selections. Paste using AND, OR, XOR or "Blend" modes. Add text, arrows, rectangles, ellipses or polygons to images.

Color Processing:

Split a 32-bit color image into RGB or HSV components. Merge 8-bit components into a color image. Convert an RGB image to 8-bit indexed color. Apply pseudo-color palettes to grayscale images.

Stacks:

Display a "stack" of related images in a single window. Process an entire stack using a single command. Open a folder of images as a stack. Save stacks as multi-image TIFF files.

* *Process>Smooth* command, 8-bit image, 3GHz Windows PC, IE 6.0, Microsoft Java 1.1.4."[4]

Preparation of Butanol Bronze:

The synthesis of the butanol bronze ink is demonstrated in the following reaction where HCl is used as a catalysis.[6]

$$CH_3CH_2CH_2CH_2OH + 4\,MoO_3 \rightarrow 2\,Mo_2O_5(OH) + CH_3CH_2CH_2C(O)H$$

Reaction 3.3. Reaction of butanol with molybdenum trioxide[6]

Preparation of the Butanol Bronze test strips to test for H_2O_2 using a video camera:

Test strips were prepared using a 0.5*u*L-10.0*u*l VWR Ergonomic High Performance pipette. Then 3.15 *u*L of butanol bronze ink was applied to each test strip pad. This was found to be the amount of material that would be just enough to completely flood each individual test strip. The next step was setting up the camera settings. Note that the camera settings had to be adjusted accordingly depending on the lightening in the room. The camera settings that worked best for the particular room we used to conduct the tests are given in Table 3.1.

Table 3.1

Camera settings used

Brightness	179
Contrast	35
Saturation	50
Sharpness	224
Backlight Compensation	1
Focus	175
LED1 mode	3

The test strips were then cut to length, fitted to a weigh boat, and taped down, in order so that the test strip would be stable through the whole video recording process. A photo of a test strip that is ready to be used for testing hydrogen peroxide is given in Figure 3.1.

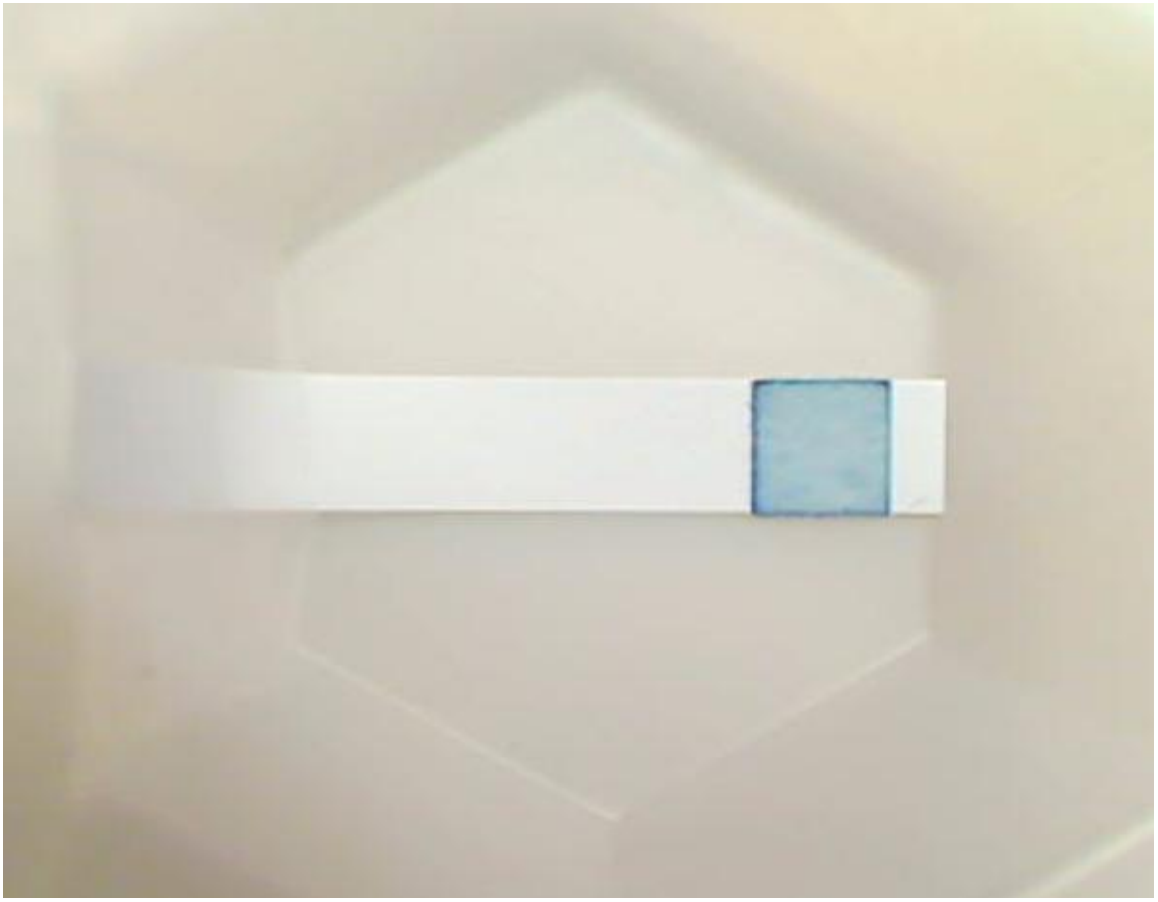

Figure 3.1. Unreacted butanol bronze test strip

After the test strip was put underneath the camera and the correct camera settings were utilized, hydrogen peroxide was then poured onto the test strip and the camera took a video of the test strip changing colors . Six different concentrations of hydrogen peroxide were used in the experiment with each concentration of hydrogen peroxide having 3 runs, with a total of 18 runs. The concentrations of hydrogen peroxide used were (in percent % H_2O_2-0.0206%, 0.0846%, 0.1208%, 0.333%, 0.9955%, and 2.88%. The hydrogen peroxide concentrations were determined through a method developed by Solvay Chemicals.[33] The video was stopped when the test strip pad turned white, as demonstrated in Figure 3.2.

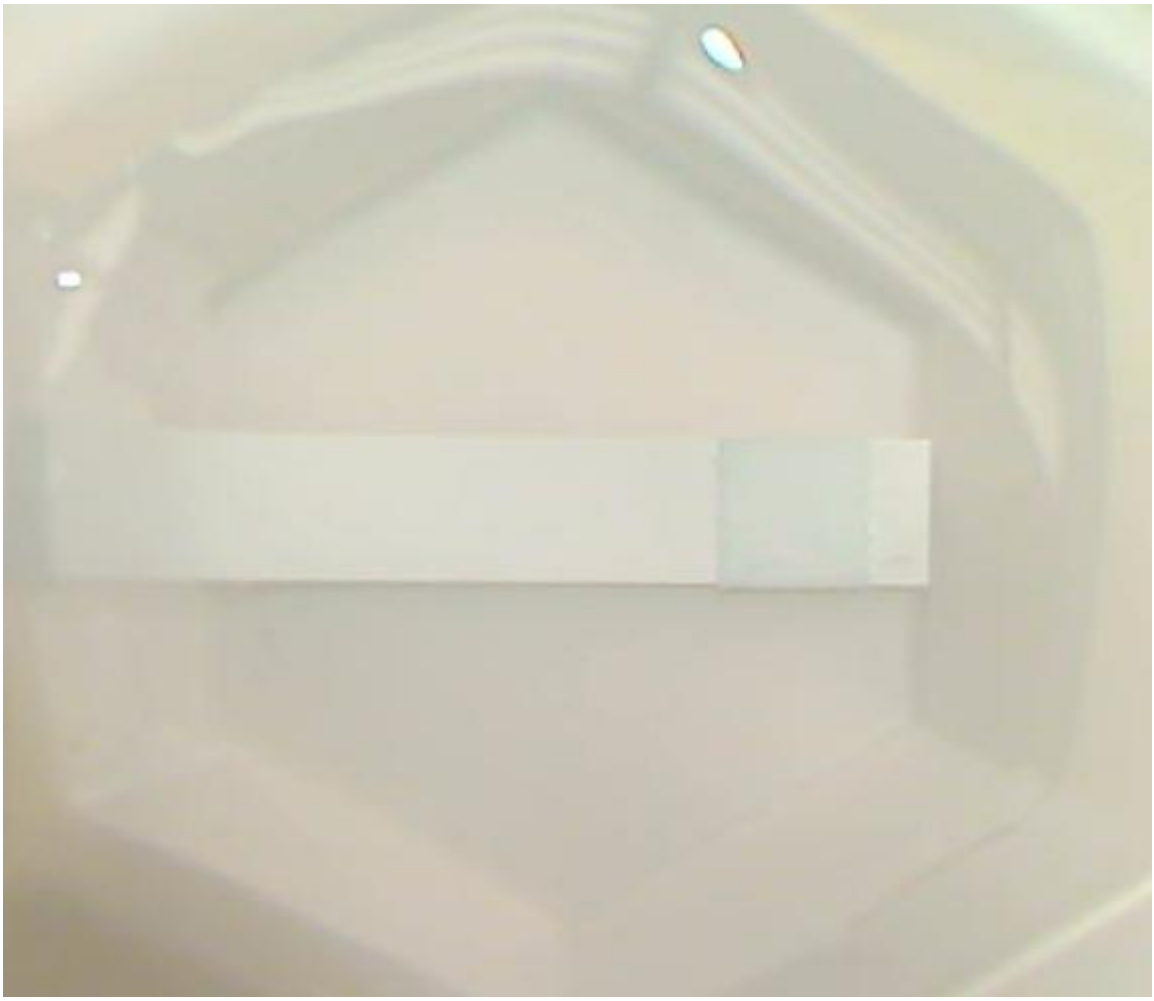

Figure 3.2. Butanol bronze test strip after reaction with H_2O_2

The butanol bronze test strips are then analyzed using the computer program ImageJ. Before using ImageJ the data must be converted to show Hoffman tables.

The command line needed to do this is " mencoder -v -noskip -ovc lavc -lavcopts gray:vcodec=mjpeg -nosound –vf framestep=15 filename.avi -o filename-new.avi". This command line gives the appropriate amount of framesteps and also insures the file has the correct Hoffman tables. The next part of analyzing the data involves putting this new file into ImageJ. The file is opened in ImageJ in grayscale format. Once the file is opened in ImageJ, go to Plugins, select "Time Series Analyzer V2.0". After this step select Auto ROI properties and

select width 20 and height 20-these are the dimensions of the box to analyze the data. The ROI-type selected should be "Rectangle". The next step was putting one of the rectangles on the pad. And one of the rectangles on the white portion of the strip. The data was now collected. ImageJ will use the white portion of the test strip as a saturation of 250-this is what is known as the "background" and the pad portion will be a number below 250, usually a number in the 100s, and this number is referred to as the "measured" portion. This step is repeated for all the test strips.

Results and Discussion of the Butanol Bronze test strips:

The purpose of this study was to see whether or not butanol bronze would make a good test strip sensor for hydrogen peroxide. The peroxide concentrations were measured by using the Solvay Chemicals, Inc. method which can be accessed online.[33] A talented undergraduate named Hayden Hanley working on his undergraduate research and titrated the hydrogen peroxide concentrations and obtained the following concentrations in Table 3.2.

Table 3.2

Concentrations of H_2O_2

Percent H_2O_2	Error Peroxide (+/-)	PPM
0.0206	**0.0002**	**206 ppm**
0.08646	**0.002172**	**864.6 ppm**
0.1208	**0.000721**	**1208 ppm**
0.333	**0.003**	**3333 ppm**
0.9955	**0.01**	**9955 ppm**
2.88	**0.01**	**28800 ppm**

Each H_2O_2 concentration was tested 3 times to ensure statistical validity. The following Figures show the first test run of each percent H_2O_2 and is shown with an overall table following all the individual Tables. Figure 3.3 shows the first test run of the 0.0206 % H_2O_2.

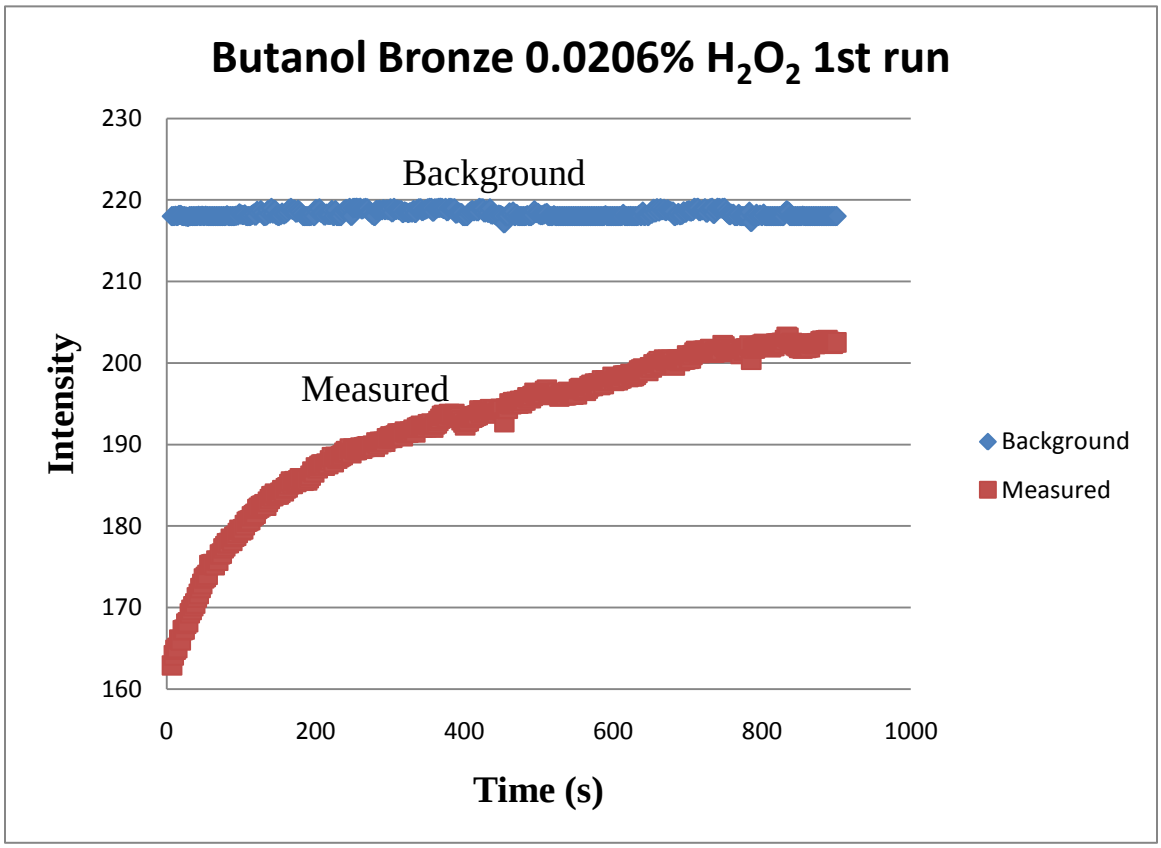

Figure 3.3. Butanol bronze 0.0206% H_2O_2 first run.

Figure 3.3 shows time (s) on the x axis and intensity of the y axis. As is expected the measured intensity approaches the background intensity over time (s). This graph also demonstrates that the butanol bronze is sensitive to H_2O_2 at 206 ppm. Figure 3.4 takes the data from Figure 3.3 and takes the natural log of the background, minus the measured value, verses time and gives a

linear plot. With a slope that is related to the rate and is $K_{observed}$.

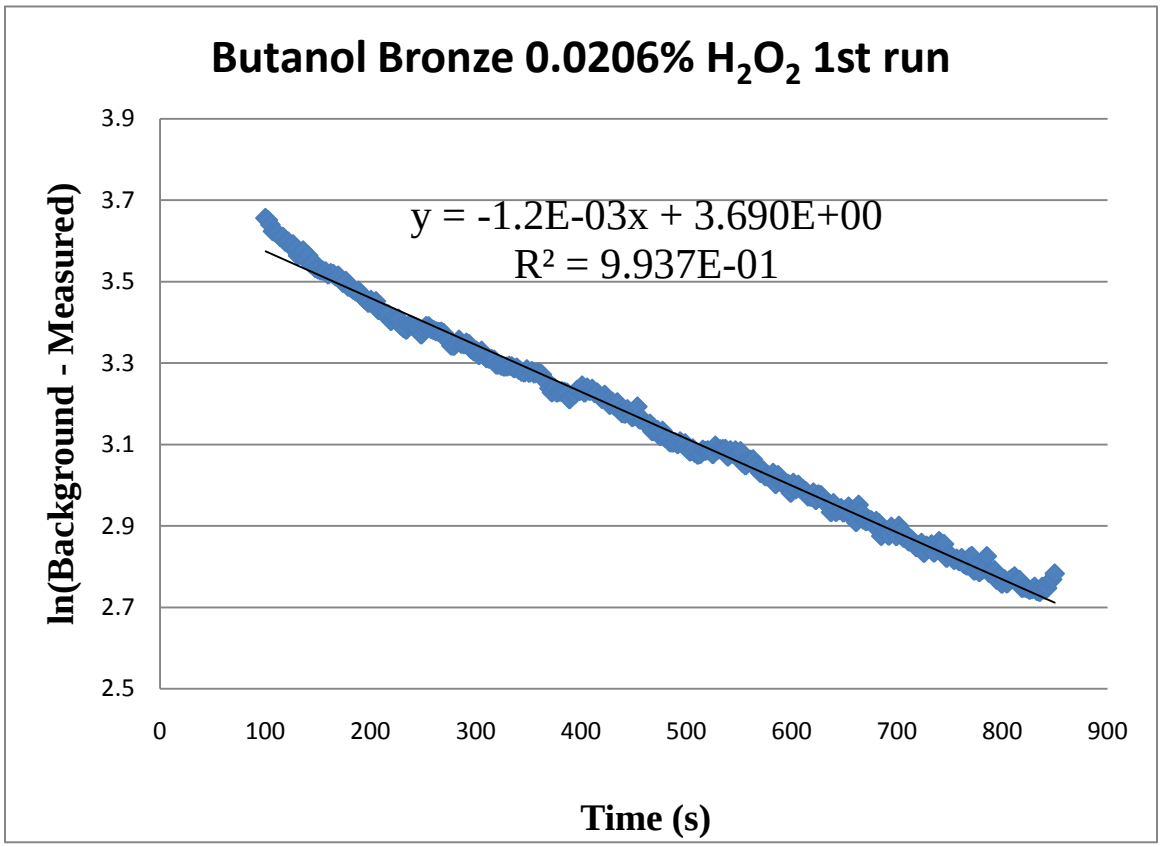

Figure 3.4. Butanol bronze 0.0206% H_2O_2 first run natural log plot

This process is then repeated for all the H_2O_2 concentrations. The intensity vs time, and the ln(Background –measured) vs time will be shown for just the 1st run's of each H_2O_2 concentration. A final plot will then be shown which averages the rate constants at a particular H_2O_2 concentration.

Figure 3.5 shows the Intensity vs Time(s) for the 0.08646 % H_2O_2.

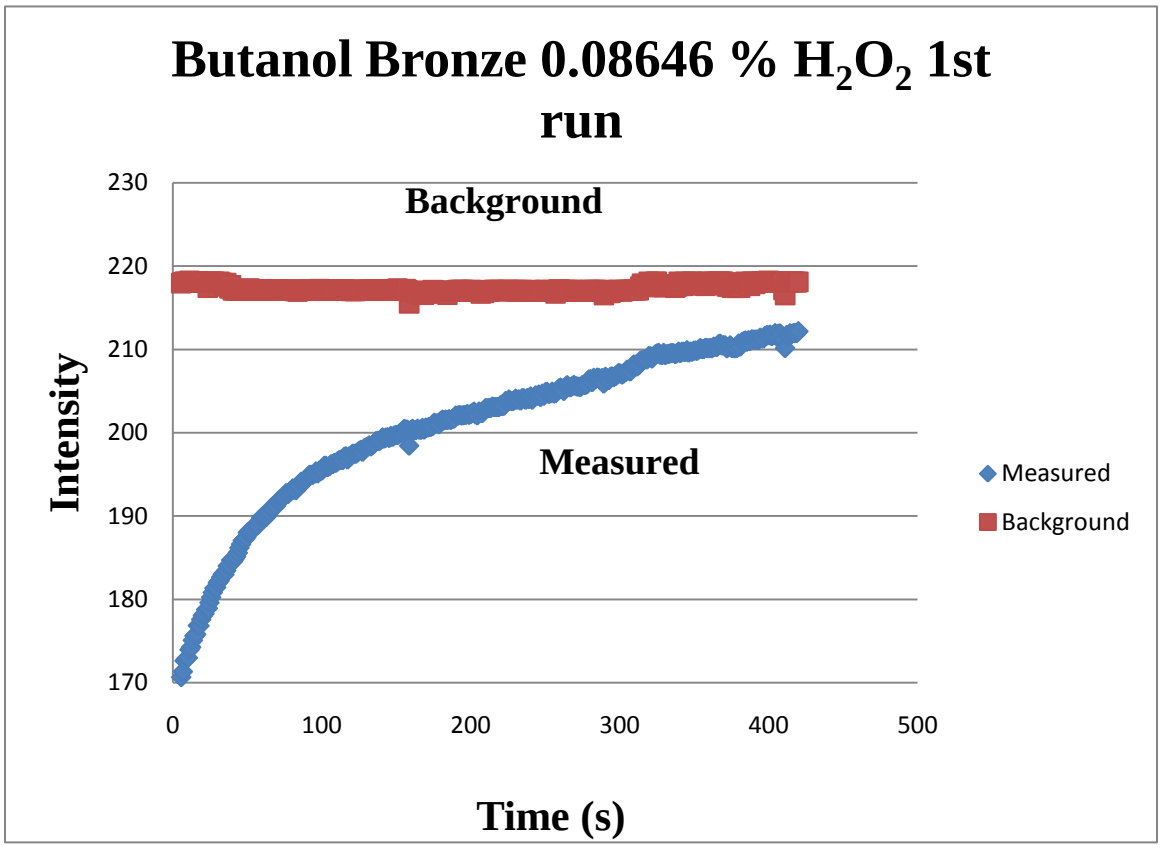

Figure 3.5. Butanol bronze 0.08646% H_2O_2 first run

Figure 3.6 shows the ln(Background-Measured) vs time for the 0.08646% H_2O_2.

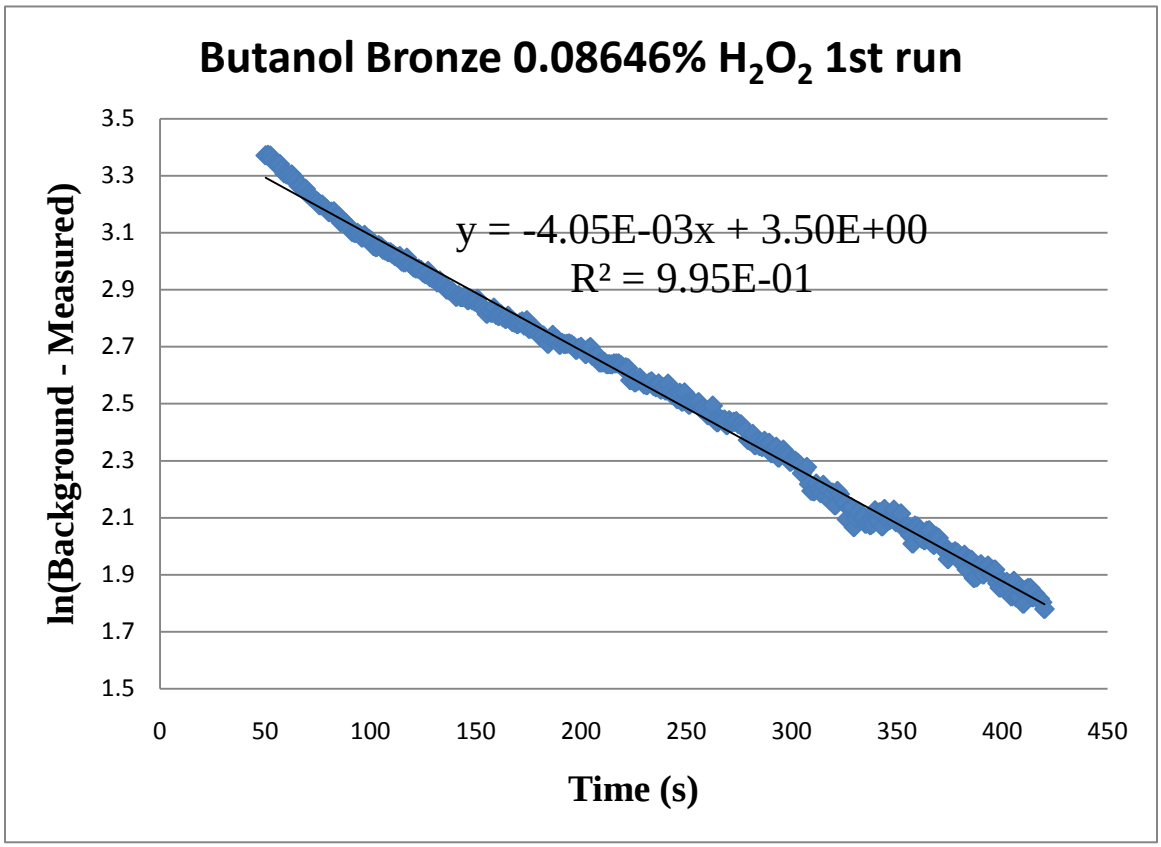

Figure 3.6. Butanol bronze 0.08646% H_2O_2 first run natural log plot

Figure 3.7 shows the Intensity vs Time(s) for the 0.1208 % H_2O_2.

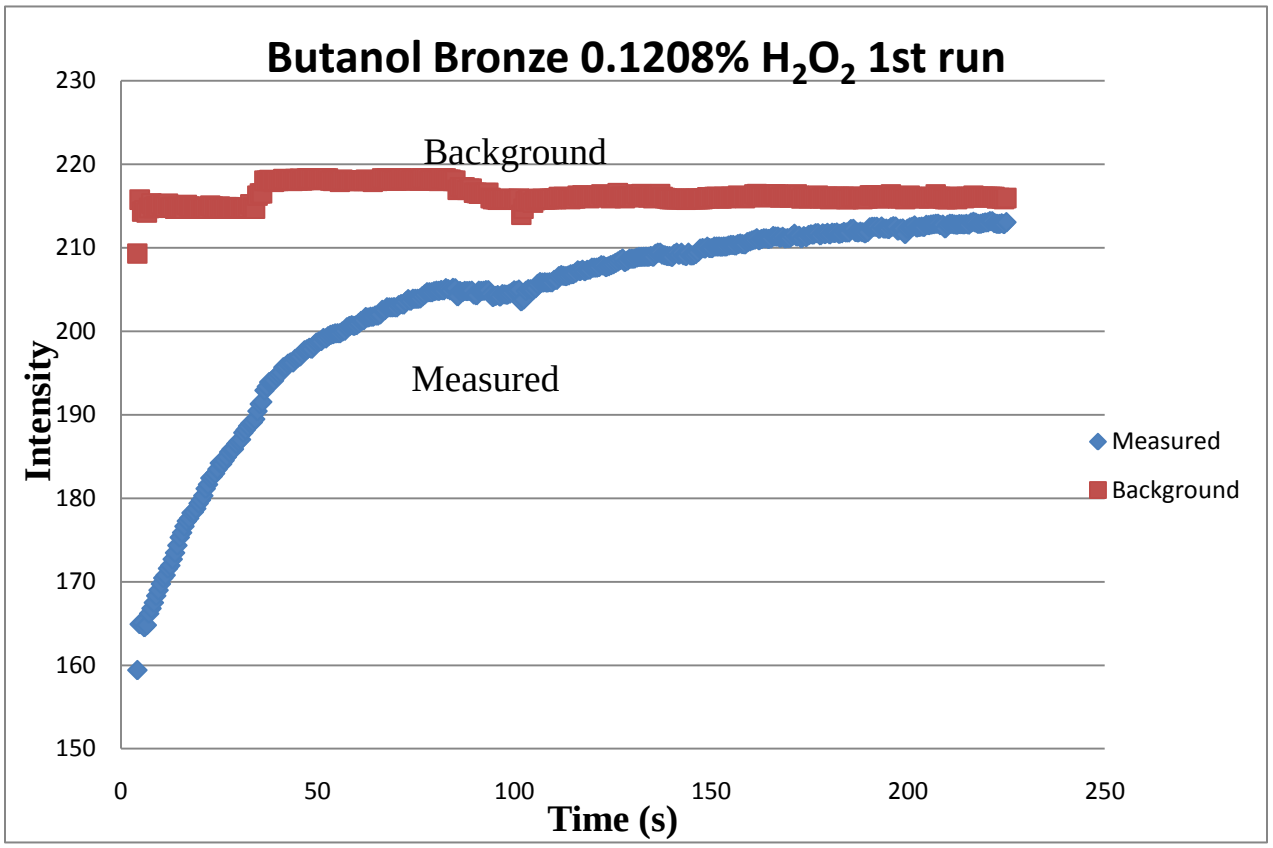

Figure 3.7. Butanol bronze 0.1208% H_2O_2 first run

Figure 3.8 shows the ln(Background-Measured) vs time for the 0.1208% H_2O_2.

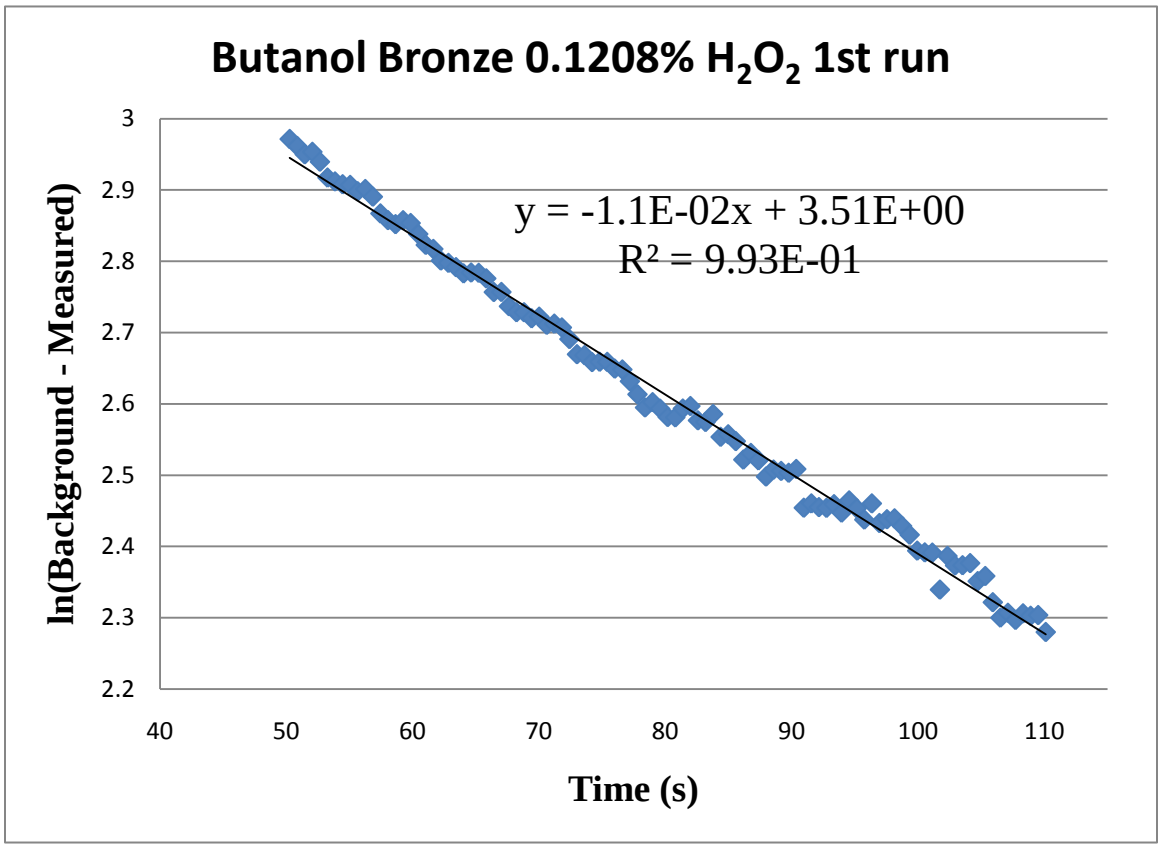

Figure 3.8. Butanol bronze 0.1208% H_2O_2 first run natural log plot

Figure 3.9 shows the Intensity vs Time(s) for the 0.333 % H_2O_2.

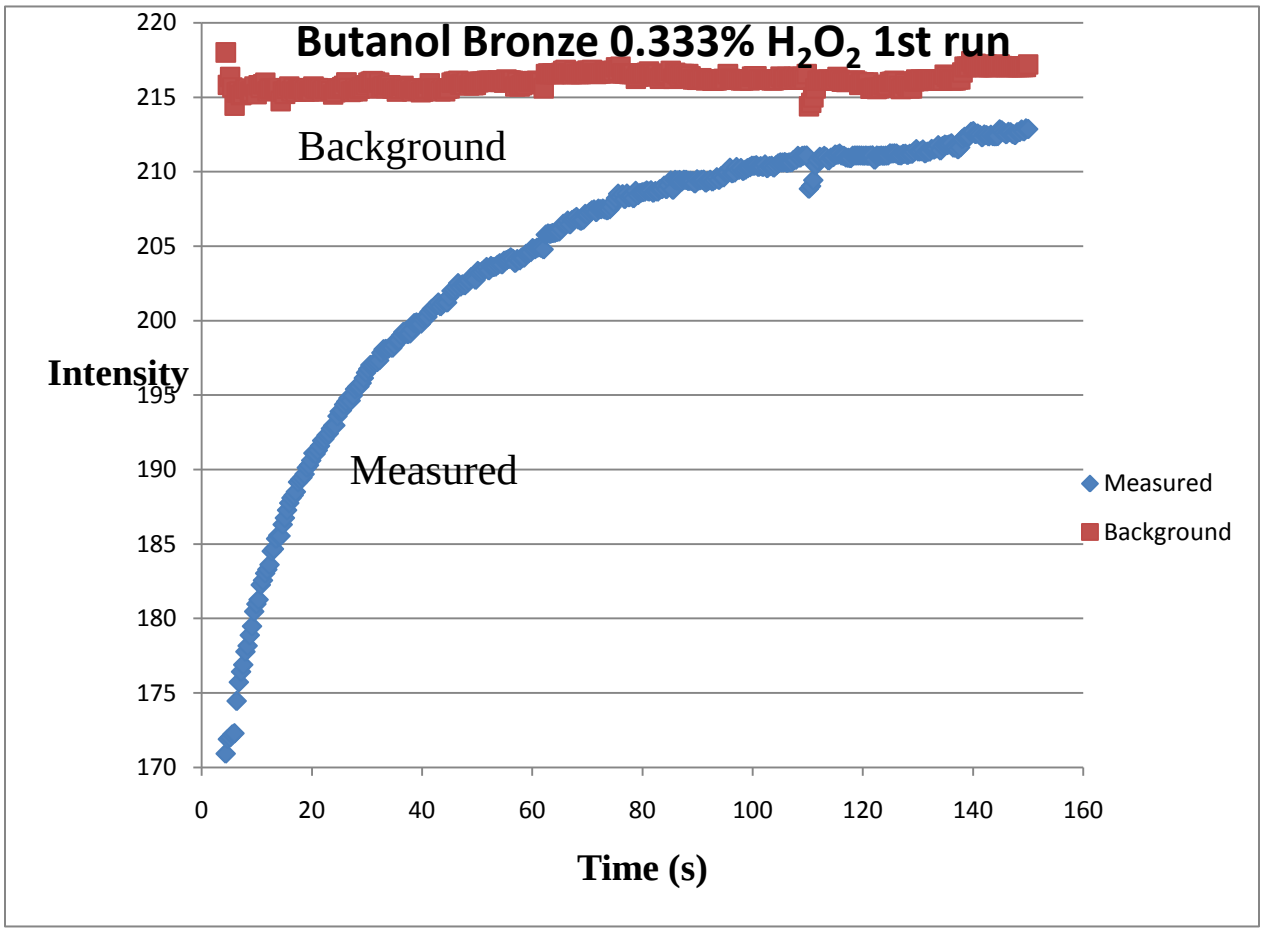

Figure 3.9. Butanol bronze 0.333% H_2O_2 first run natural log plot

Figure 3.10 shows the ln(Background-Measured) vs time for the 0.333% H_2O_2.

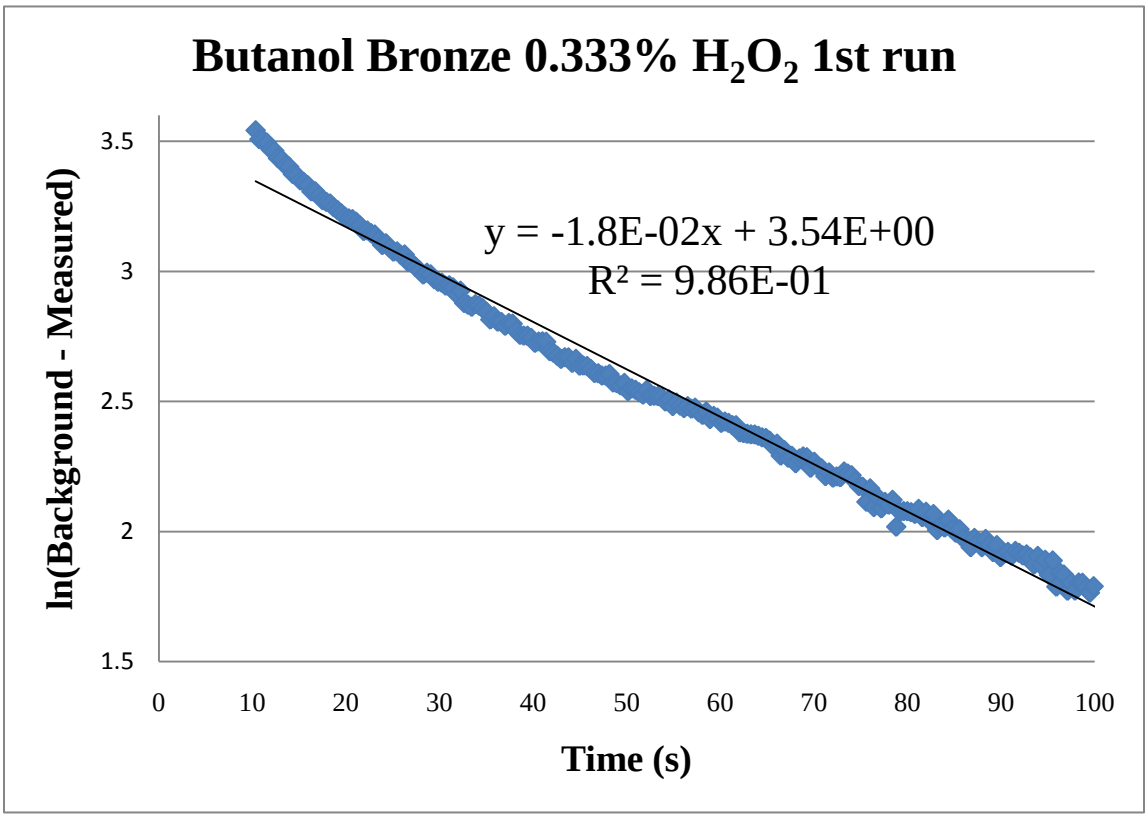

Figure 3.10. Butanol bronze 0.333% H_2O_2 first run natural log plot

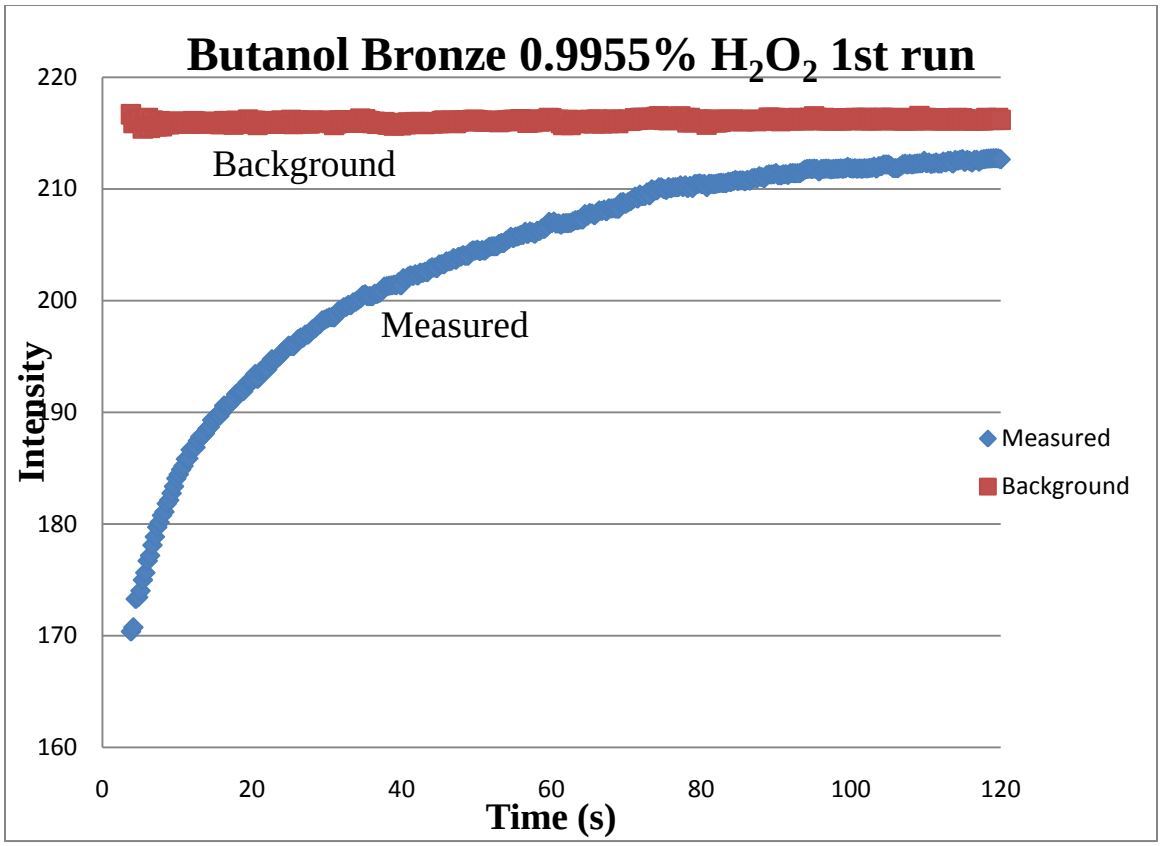

Figure 3.11. Butanol bronze 0.9955% H_2O_2 first run

Figure 3.12 shows the ln(Background-Measured) vs time for the 0.9955% H_2O_2.

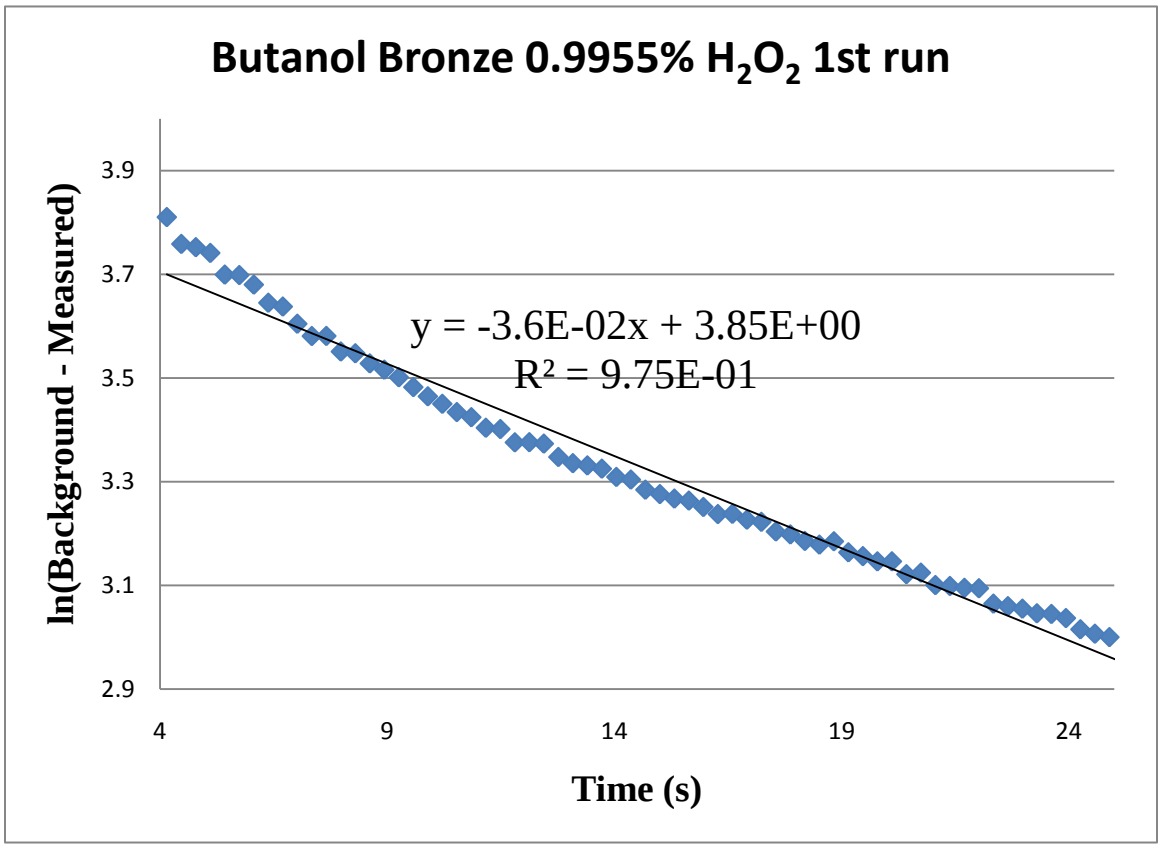

Figure 3.12. Butanol bronze 0.9955% H_2O_2 first run natural log plot

Figure 3.13 shows the Intensity vs Time(s) for the 2.88 % H_2O_2.

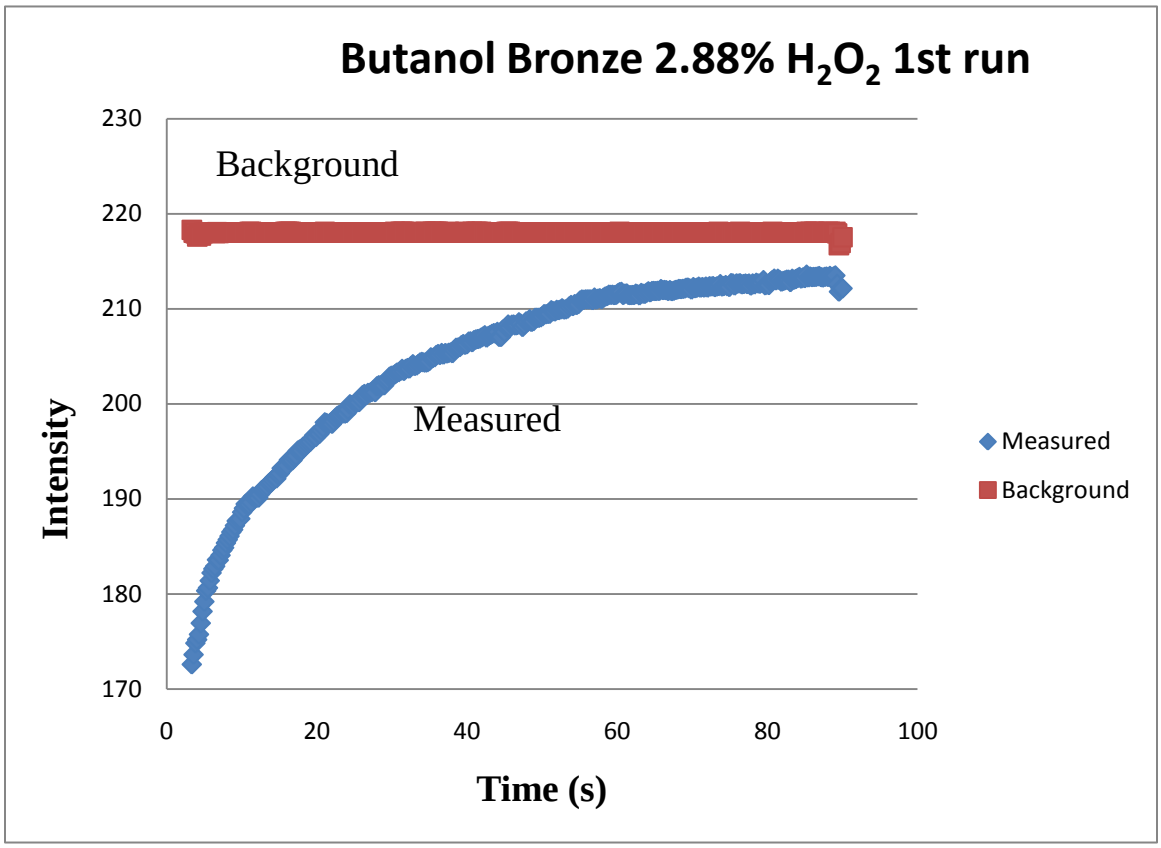

Figure 3.13. Butanol bronze 2.88% H_2O_2 first run

Figure 3.14 shows the ln(Background-Measured) vs time for the 2.88% H_2O_2.

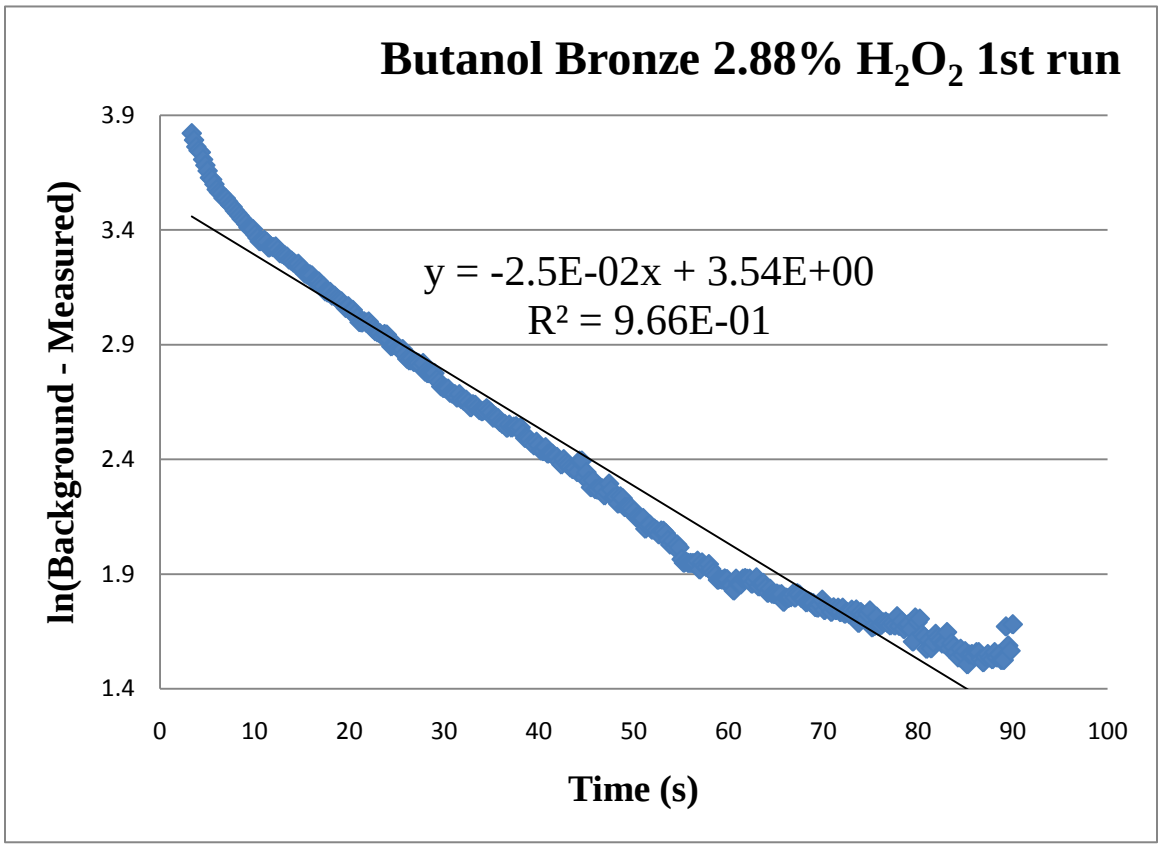

Figure 3.14. Butanol bronze 2.88% H_2O_2 first run natural log plot.

Table 3.3 summarizes all of the above data and includes all three runs per H_2O_2 concentration.

Table 3.3

Summarized data of butanol bronze

Average Rate Constant	Standard Deviation	H_2O_2 %	mol/L
1.07E-03	6.81E-05	0.0206	6.06E-03
4.82E-03	9.28E-04	0.08646	2.54E-02
9.4E-03	1.25E-03	0.1208	3.55E-02
1.95E-02	2.08E-03	0.333	9.79E-02

A software program called sigma plot was then utilized. Figure 3.15 shows the Rate Constant vs. H_2O_2(mol/l).

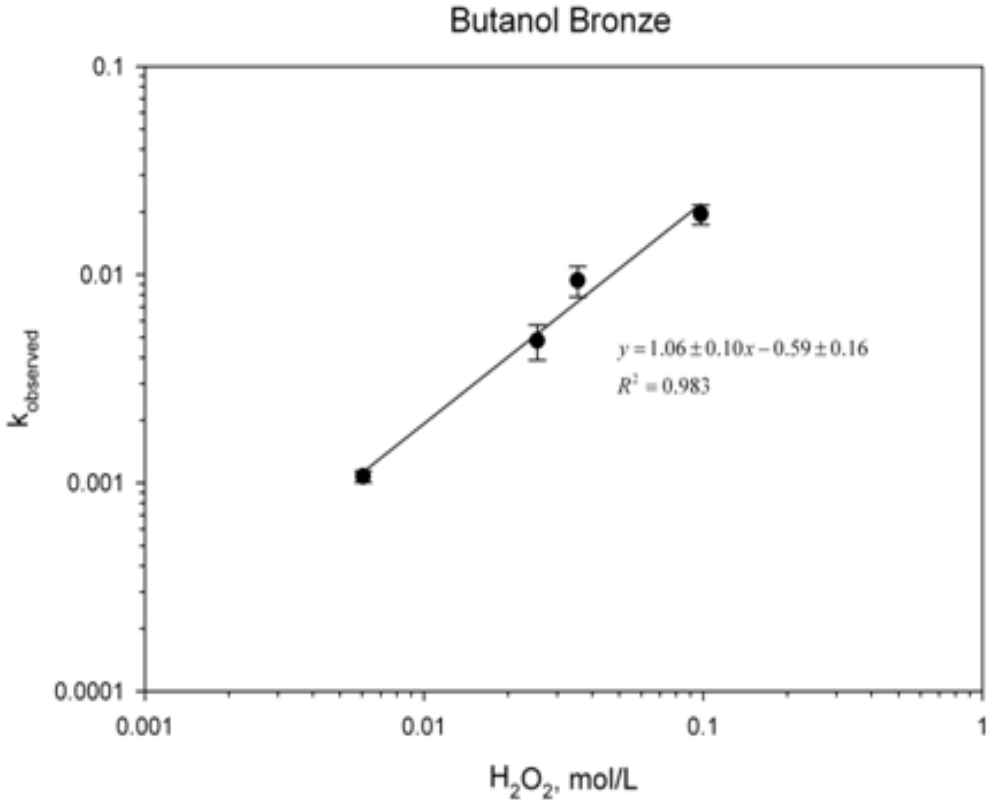

Figure 3.15. $K_{observed}$ vs H_2O_2 mol/L

From the plot, the butanol bronze is first order in H_2O_2. Since $K_{observed}=k[H_2O_2]$, we can calculate k.

Table 3.4

$K_{average}$

Moles / Liter	K_{obs}	k	k average
8.47E-01	2.36E-02	2.81E-02	2.57E-01
2.93E-01	2.55E-02	9.38E-02	
9.79E-02	1.95E-02	2.29E-01	
3.55E-02	9.40E-03	3.23E-01	
2.54E-02	4.82E-03	2.36E-01	
6.06E-03	1.07E-03	2.41E-01	

$K_{average}$ is 2.6E-01 L mol^{-1} $second^{-1}$.

An ultra violet spectrum was taken of the above butanol bronze using the Carey 5000. The Carey 5000 was utilized since we wanted to see the shoulder region in the near infrared region. Figure 3.16 shows the ultra violet spectrum of the butanol bronze.

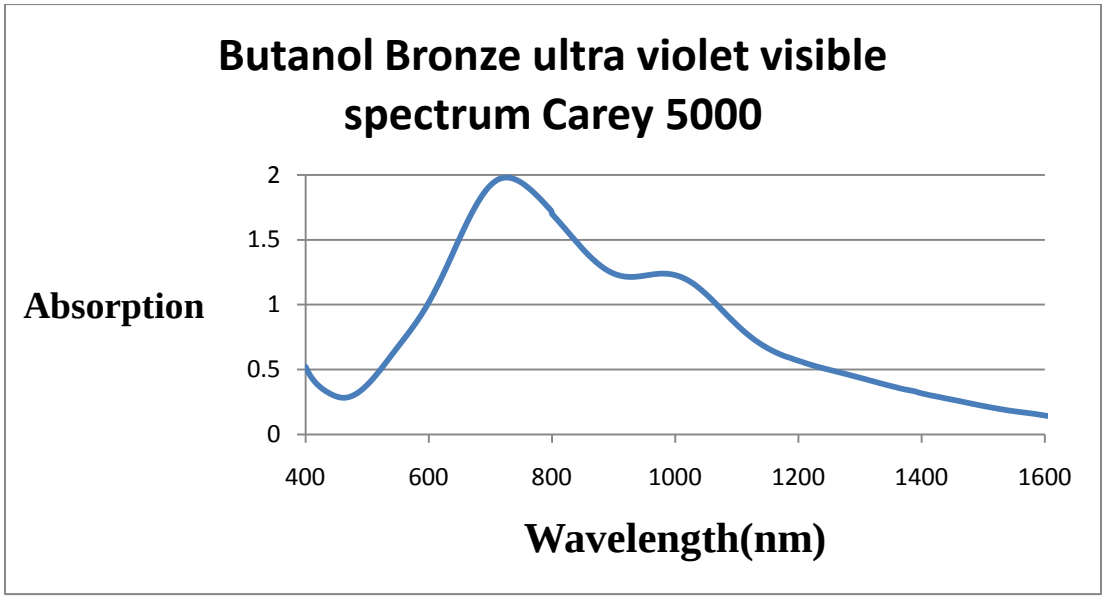

Figure 3.16. Butanol bronze ultraviolet spectrum

The butanol bronze was also showed to be nanometric by dynamic light scattering as is shown in Figure 3.17, with a diameter of 1.34 nanometers.

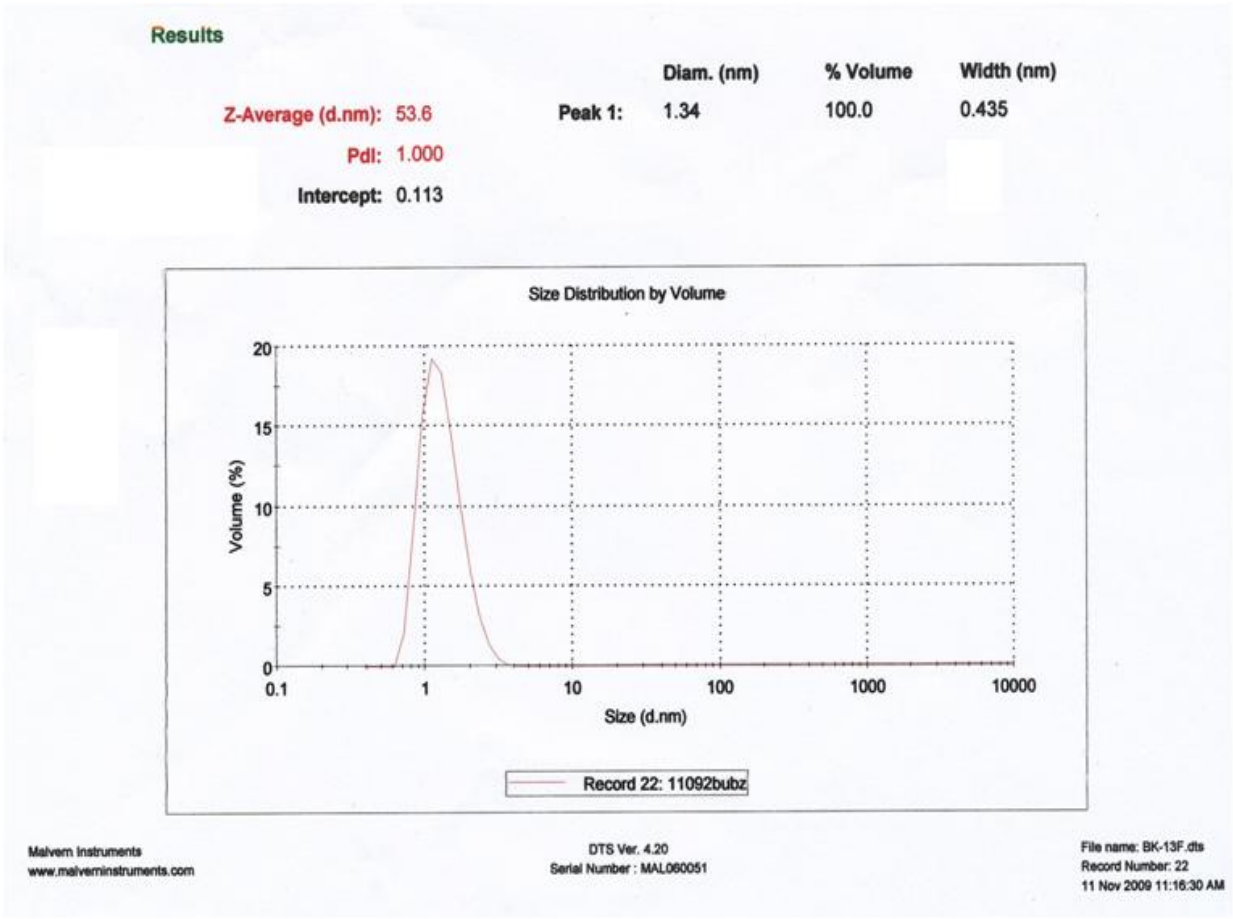

Figure 3.17. Dynamic light scattering of butanol bronze

Conclusions

The hydrogen bronze synthesized from the above reaction proved to be an effective material when used to test for the sensibility of H_2O_2. The material is also nanometric in size as the corresponding dynamic light scattering would indicate. The blue bronze material proved to be an effective reducing agent and future studies will look at more of a green chemistry side to be studied since the blue ink synthesized in this chapter required butanol.

CHAPTER IV

Sodium Gluconate, Molybdenum Trioxide, and Water as an Enviromental Green Solvent

Purpose:

The purpose of this chapter is to use green chemistry, i.e. a water based solvent, to make an effective sensing agent just like in chapter III. Chapter III utilized a butanol- based solvent. The solvent of choice here will be much more environmentally friendly, and the sensor will prove to be a better sensor at detecting peroxides as this chapter will show. The chemicals of choice in synthesizing the sodium gluconate molybdenum dimer will be sodium gluconate, molybdenum trioxide, and deionized water. This chapter also will demonstrate that by using different mole ratios of sodium gluconate:molybdenum trioxide, a whole new complex can be formed unrelated to the blue dimerized complex synthesized that will be used for the test strips.

Experimental:

All chemicals were reagent grade (ACS reagent grade) and were utilized without further purification. Ultra Violet spectrum were characterized using a [Carey 50]. The camera work was

done using Dr. Materer's lab camera and then utilizing the program ImageJ from the National Institute of health to analyze the kinetic data.

Preparation of Sodium Gluconate Molybdenum dimer:

A 500 ml round bottom flask was charged with 23.984 g of MoO_3(166.69 mmol), 18.183 g of sodium gluconate(83.28 mmol), and 250 ml of deionized water. A stir bar was also added to the round bottom flash for proper mixing. The reaction is then refluxed for 19.5 hours. After 19.5 hours the reaction is done and is allowed to cool to room temperature. The blue ink is then separated from the residual solids by using a fine sintered-glass filter funnel and the ink is then placed in a 250 ml media bottle. The residual solids are then dried in a vacuum oven at room temperature and stored in a glass or plastic scintillation vial. The weight of the residual solids left over is around 7.85 grams. Therefore out of the original 23.984 g of MoO_3 that was utilized in the reaction around 16.13 grams of MoO_3 are actually used in the reaction or a reaction ratio of 1.35:1.00 MoO3 to sodium gluconate.

Preparation of the 2:1 Sodium Gluconate, Molybdenum Trioxide Complex:

All chemicals were reagent grade (ACS reagent grade) and were utilized without further purification. 20 millimoles(4.36 grams) of sodium gluconate, 10 millimoles(1.44 grams) of molybdenum trioxide, and 100 grams of dionized water were charged to a 250 ml beaker and was heated and stirred until all contents went into solution. The solution was then cooled to room temperature. Further purification was done using 95 percent ethanol, and absolute ethanol to remove the impurities by centrifugation, and a yellow solid was left over. The yellow solid was characterized using nuclear magnetic resonance, infra-red spectroscopy, and raman spectroscopy. The NMR spectroscopy was run in D_2O using a Varian UNITY INOVA 400. Infra-red

spectroscopy was done using a Magna-IR spectrometer 750 Nicolet, and raman spectroscopy was done using a Nicolet NXX 9610.

Reaction 4.1 shows the reaction scheme.

$$2NaGluconate + 1MoO_3 \rightarrow 2Na^{1+} + MoO_2(gluconate)_2^{2-}$$

Reaction 4.1. Reaction of sodium gluconate with molybdenum trioxide.

Results and discussion:

Similar to chapter 3 ImageJ was utilized in determining the order of H_2O_2, and the $K_{observed}$ of the reaction at a particular concentration of H_2O_2. Table 4.1 shows the H_2O_2 percents used in the experiment.

Table 4.1

H_2O_2 concentrations

Percent H_2O_2	Error Peroxide (+/-)	PPM
0.0206	0.0002	206 ppm
0.08646	0.002172	864.6 ppm
0.1208	0.000721	1208 ppm
0.333	0.003	3333 ppm
0.9955	0.01	9955 ppm
2.88	0.01	28800 ppm

Figure 4.1 shows a photograph of the blue ink applied to a test strip, Figure 4.2 shows a photograph of the blue ink after reacting with H_2O_2.

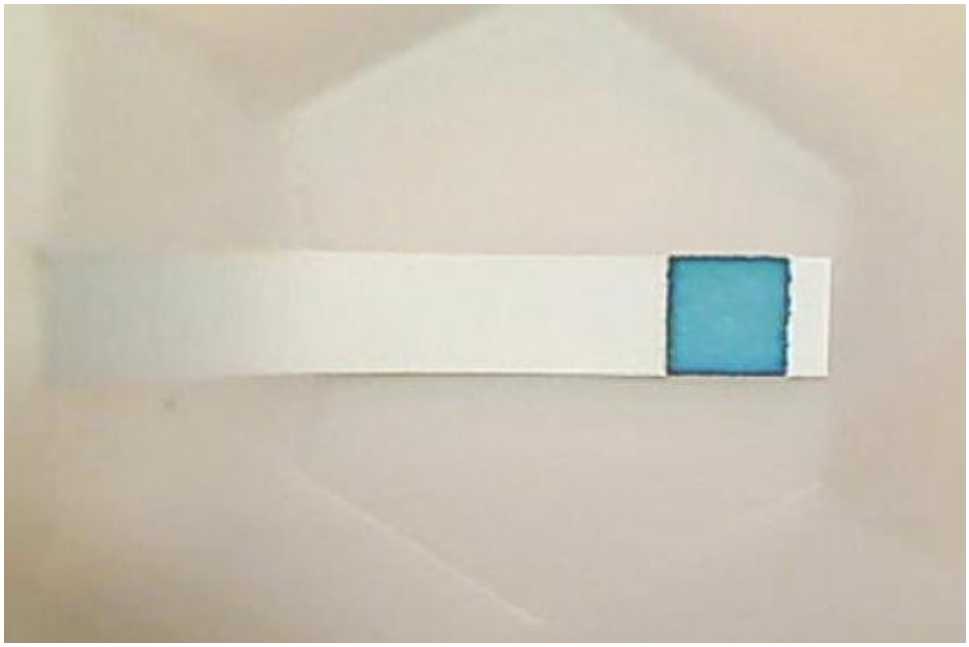

Figure 4.1. Unreacted blue sodium gluconate test strip

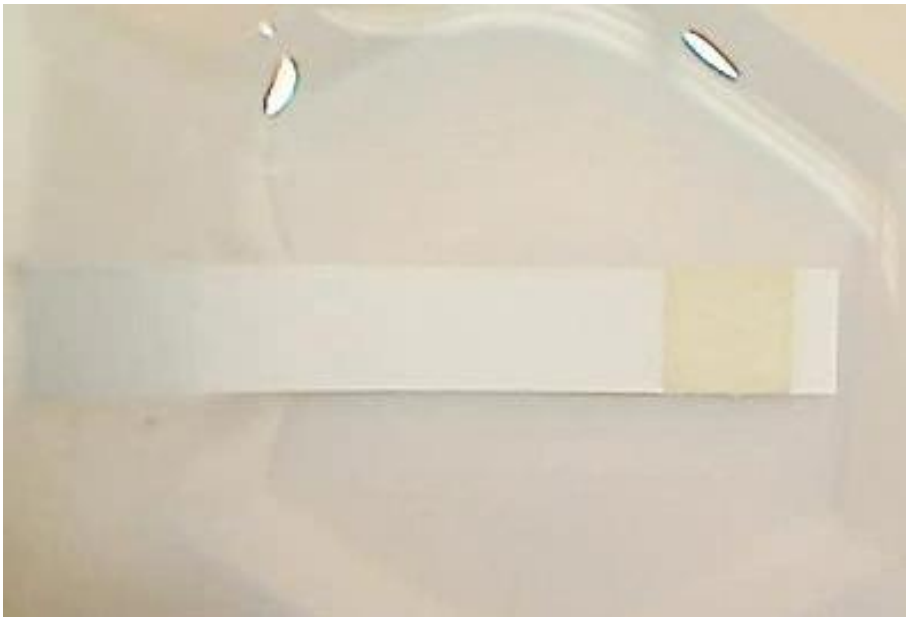

Figure 4.2. Blue sodium gluconate test strip after reacting with H_2O_2

As was observed in chapter 3 utilizing ImageJ, plots of the intensity vs. time will show that the test strip material is effective at detecting H_2O_2 at very small concentrations of H_2O_2. The smallest percent peroxide that was tested was 206 ppm. Each peroxide run was tested three different times. The first run of each concentration of H_2O_2 will be shown, and a master chart showing the average of the three runs will lastly be shown.

Figure 4.3 shows the percent H_2O_2 for 206 ppm of intensity vs time(s). As will be shown in all the following graphs, the measured will approach the background.

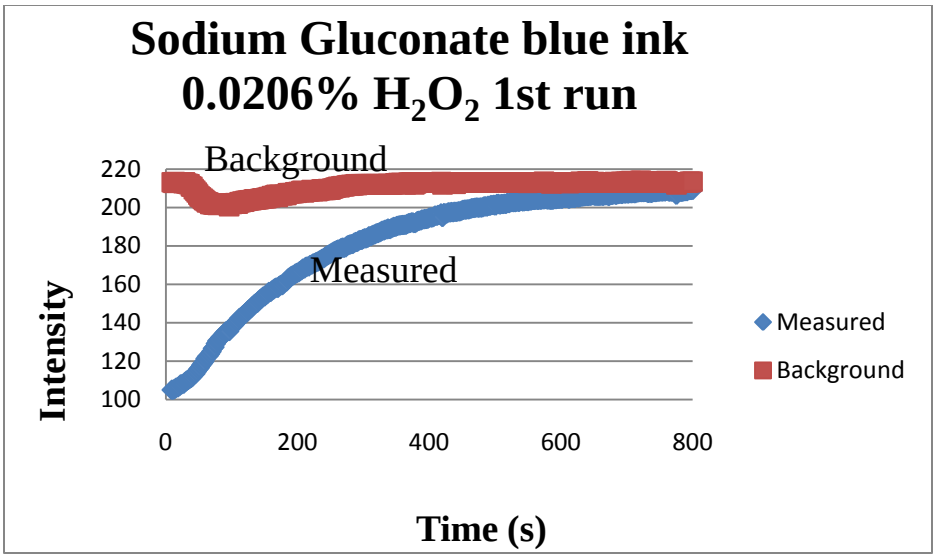

Figure 4.3. Sodium gluconate blue 0.0206% H_2O_2 first run

Figure 4.4 shows the ln(background-measured) and gives a linear correlation with time, the slope represents $k_{observed}$.

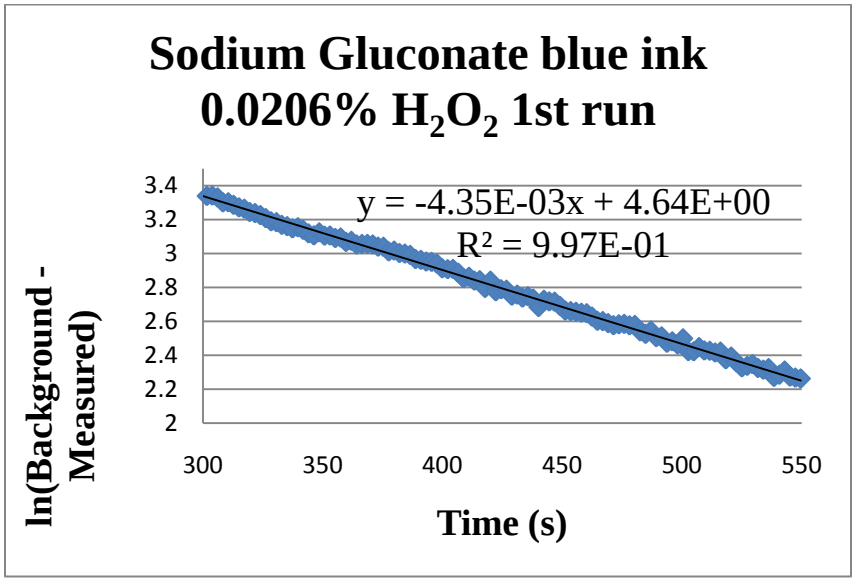

Figure 4.4. Sodium Gluconate blue 0.0206% H_2O_2 first run ln plot

Figure 4.5 shows the percent H_2O_2 for 1208ppm of intensity vs time(s).

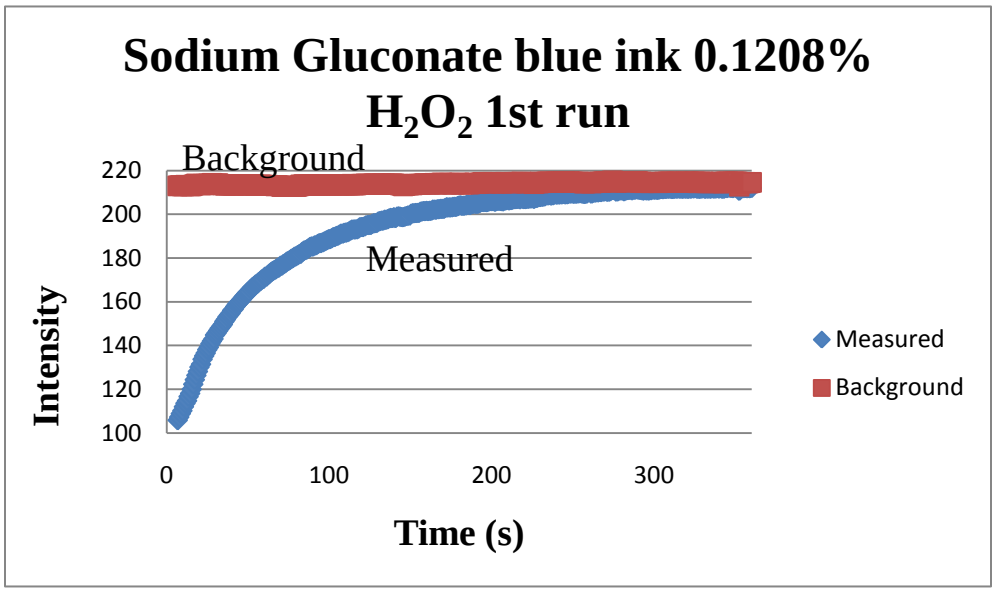

Figure 4.5. Sodium Gluconate blue 0.1208% H_2O_2 first run plot

Figure 4.6 shows the ln(background-measured) and gives a linear correlation with time, the slope represents $k_{observed}$.

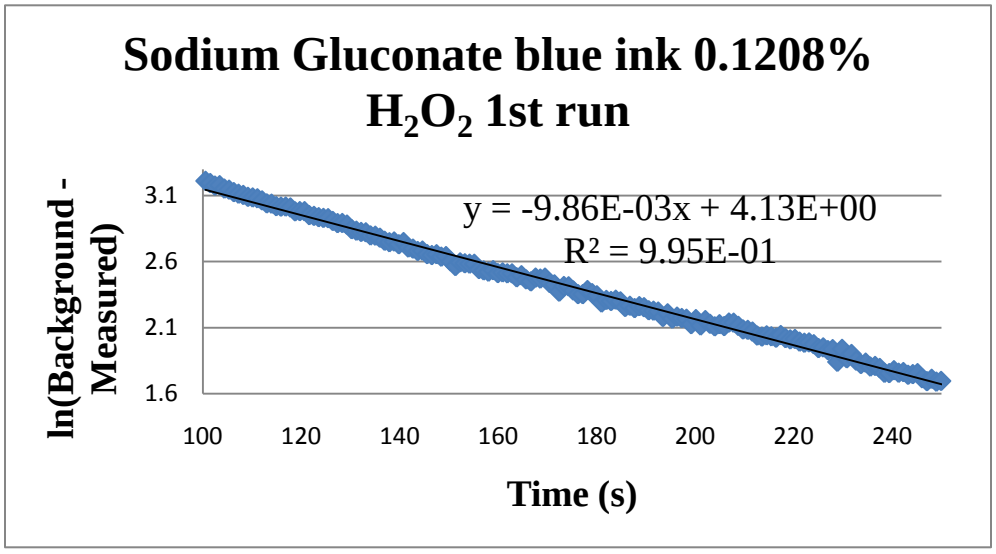

Figure 4.6. Sodium Gluconate blue 0.1208% H_2O_2 first run ln plot.

Figure 4.7 shows the percent H_2O_2 for 3333ppm of intensity vs time(s).

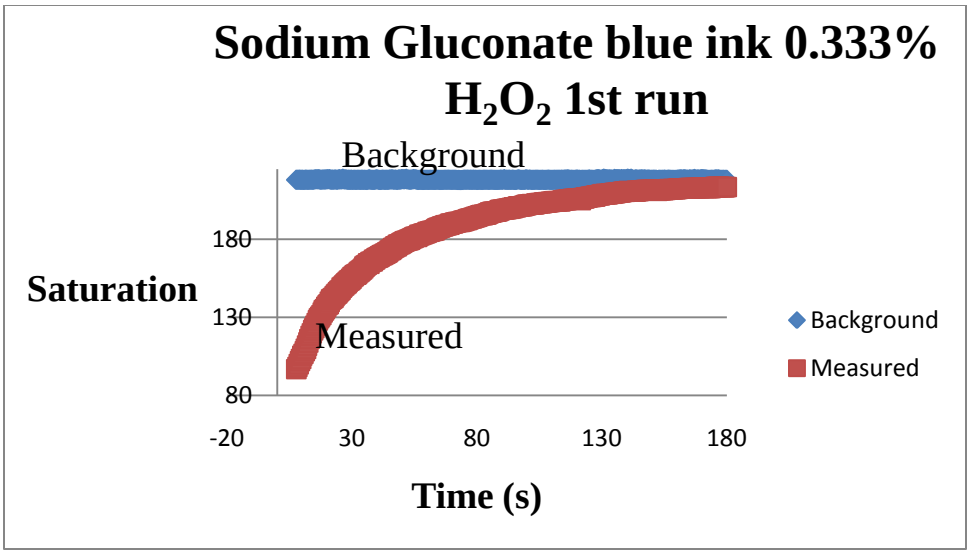

Figure 4.7. Sodium Gluconate blue 0.333% H_2O_2 first run plot.

Figure 4.8 shows the ln(background-measured) and gives a linear correlation with time, the slope represents $k_{observed}$.

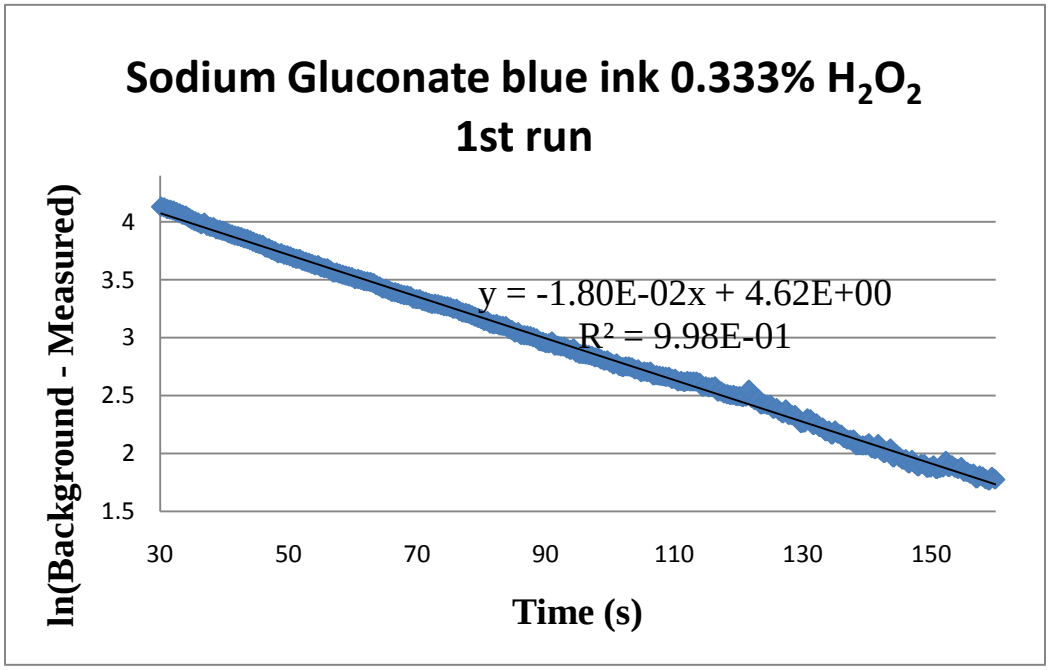

Figure 4.8. Sodium Gluconate blue 0.333% H_2O_2 first run ln plot.

Figure 4.9 shows the percent H_2O_2 for 9955 ppm of intensity vs time(s).

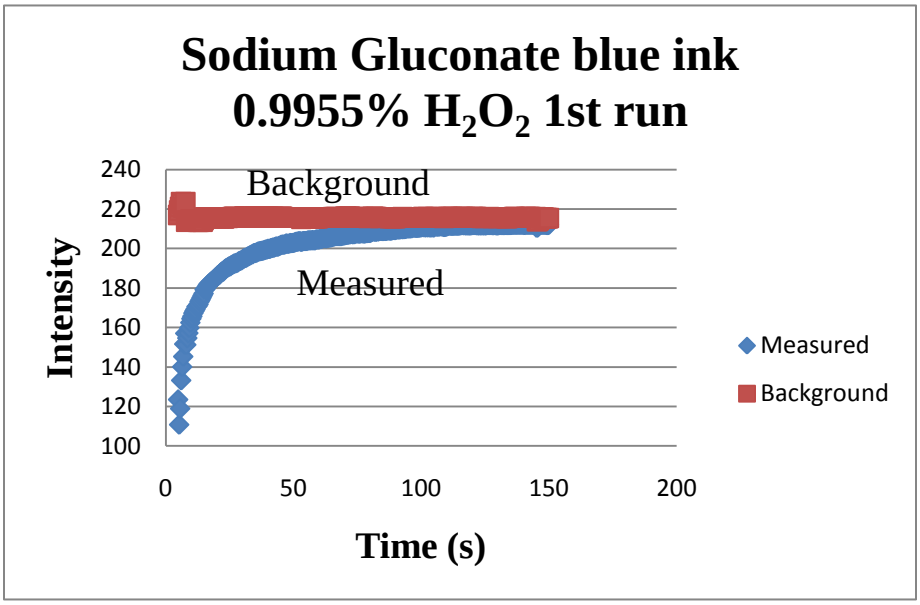

Figure 4.9. Sodium Gluconate blue 0.9955% H_2O_2 first run plot.

Figure 4.10 shows the ln(background-measured) and gives a linear correlation with time, the slope represents $k_{observed}$.

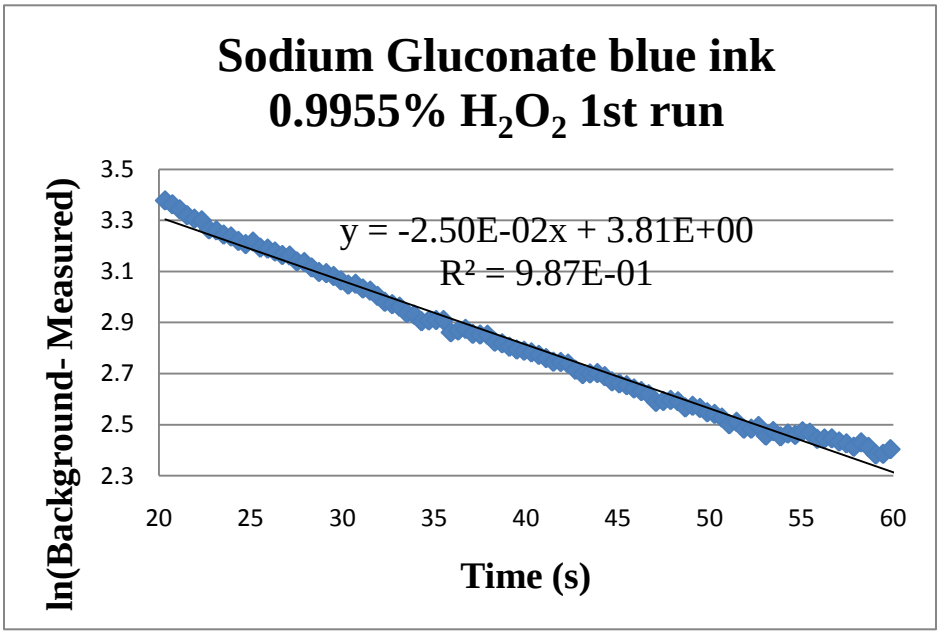

Figure 4.10. Sodium Gluconate blue 0.9955% H_2O_2 first run ln plot.

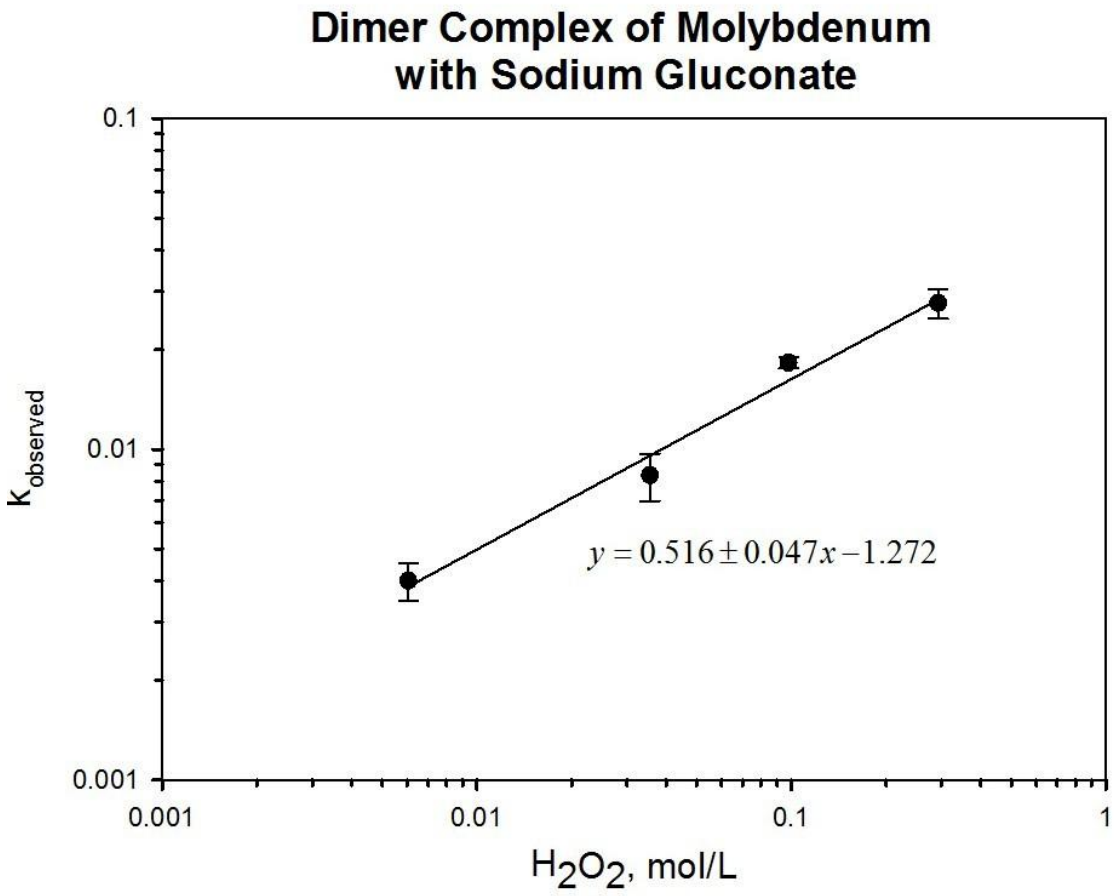

Figure 4.11. $K_{observed}$ vs H_2O_2 mol/L.

Figure 4.11 is a plot that shows $k_{observed}$ vs the concentration of H_2O_2. From the slope the reaction is half order in H_2O_2 where as was the case for the butanol bronze was first order in H_2O_2. The case can be seen again if the blue ink is diluted up to 50 percent with deionized water. Figure 4.12 shows that the same half order in H_2O_2 is again observed.

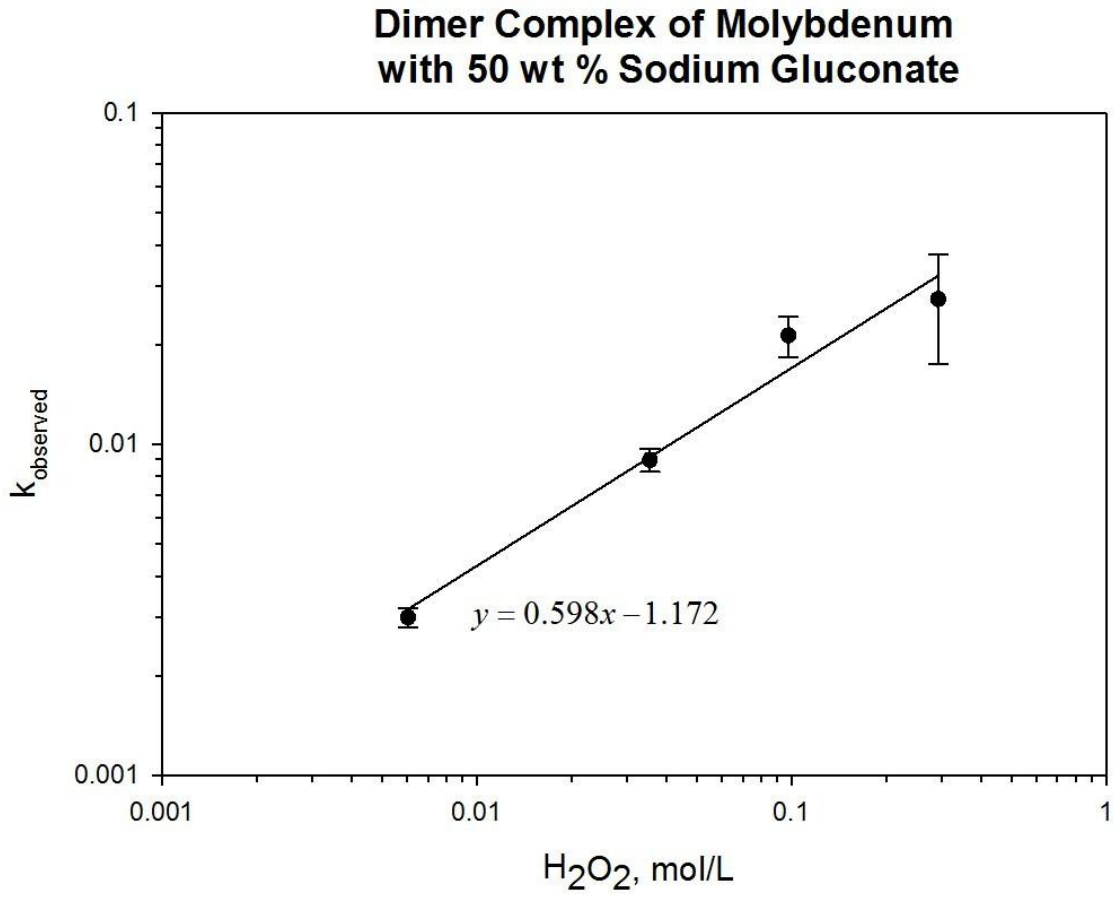

Figure 4.12. 50% weight by dilution, $K_{observed}$ vs H_2O_2 mol/L.

Using the equation $K_{obs}=k[H_2O_2]^X$, k can easily be calculated, and k comes out to be 4.1×10^{-2} $L^{-1/2}$ $mole^{-1/2}$ sec^{-1}.

A ultra-violet visible spectrum was taken with the Varian cary 50, and is shown in Figure 4.13. It should be noted the ultra-violet visible spectrum was taken in a 1.0 cm. pathlength cuvette, and was diluted to a 1 and 10 concentration with deionized water.

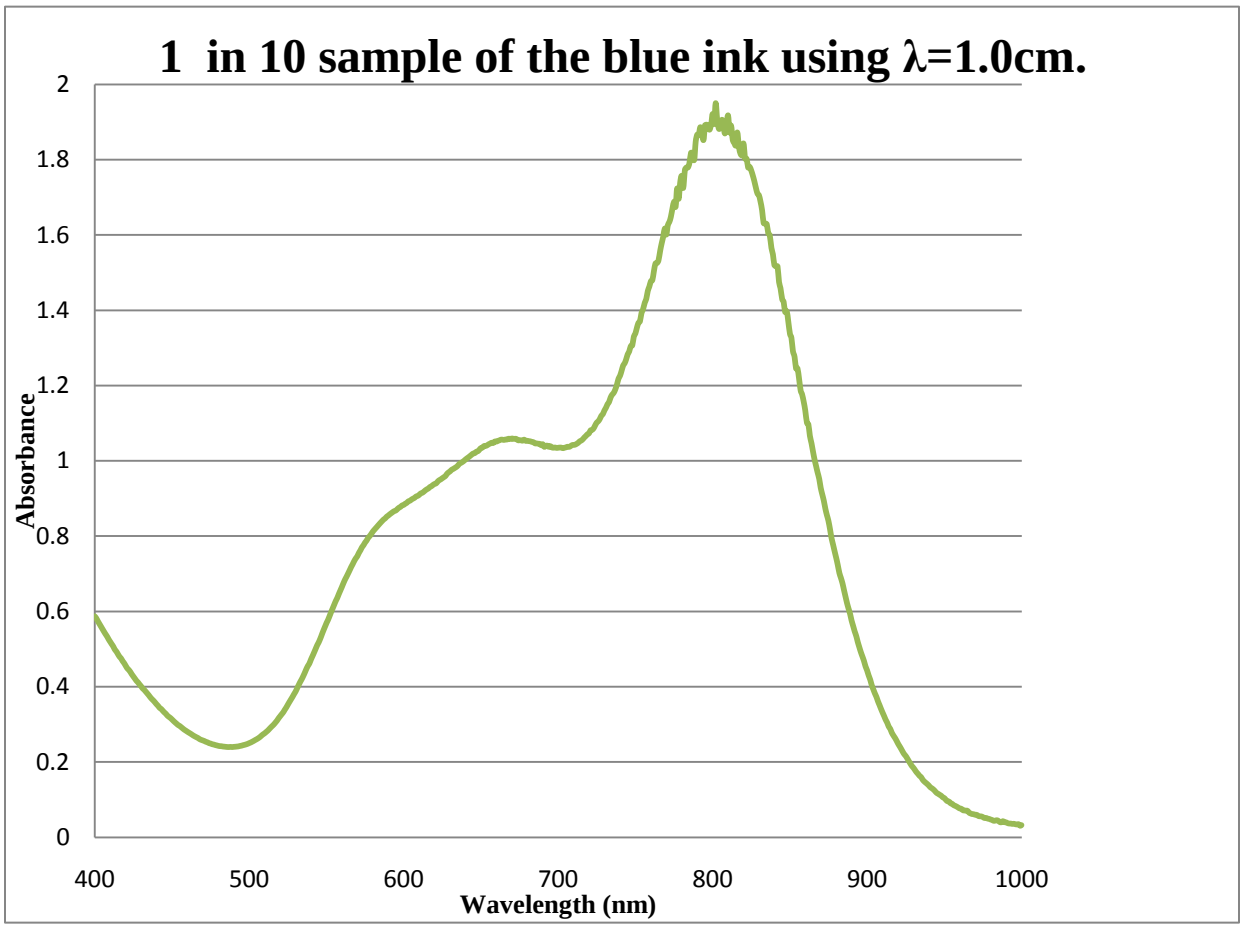

Figure 4.13. Ultraviolet visible spectrum of the sodium gluconate blue ink.

It should also be noted that there is an optimal reflux time for the reaction to give an optimal absorbance, which is demonstrated in Figure 4.14.

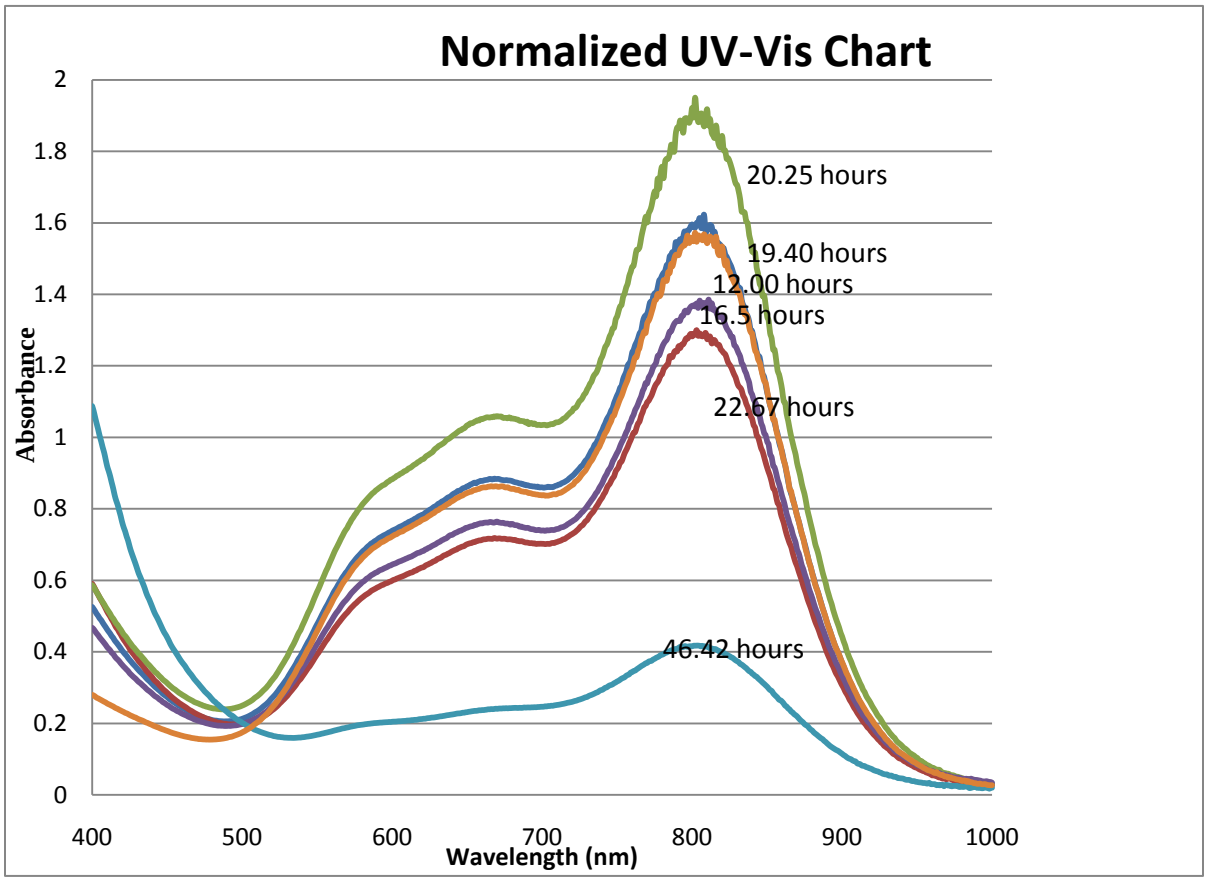

Figure 4.14. Normalized ultra-violet visible spectrum at various times.

Figure 4.14 shows the 2.0 molybdenum trioxide to 1.0 sodium gluconate dimerized blue ink complexe ultra violet spectrums. The difference being is the reaction times. If the reaction vessel refluxes beyond 20 hours the absorbance is not at a maximum, which can be seen with the 46.42 hour run. Also if the reflux is not run long enough as the 12.00 hr, and 16.5 hr. reflux times show we did not hit an optimal absorbance. If the reaction goes between 19.5 and 20.5 hours that proved to give a maximum absorbance.

This complex really mystified us in the beginning since at very low concentrations we would start off with a blue complex that would shift to a yellow/clear complex indicating that we had Mo^{VI}.

On a whim I put the colorless solution that was once blue in a regrigerator and the complex turned blue. This was later confirmed through experiments where I heated up a sealed cuvette and the solution would turn from blue to green to yellow. And when the solution was allowed to cool back to room temperature the solution turned back blue again. The equilibrium that we postulated was that we had a dimer that was in equilibrium with two monomers.

$$\mathbf{Mo^{V}\text{-}Mo^{VI}} \quad \rightleftharpoons \quad \mathbf{Mo^{V} + Mo^{VI}}$$

colorful Dye **clear yellow**

Scheme 4.1. Dimer complex in equilibrium.

This equilibrium can be seen by 3 experiments that I set up using the Varian cary 5000 to do temperature controlled kinetics with. The experiment consisted of taking 100 percent pure concentrate blue ink made from the procedure in chapter 4, putting it in a 1.0 cm sealed cuvette, and running temperature controlled kinetics at three different temperatures. The temperatures chosen for these sets of experiments were 0, 70, and 80 ^{o}C. It should be noted that each temperature was run 3 times and λ was chosen to be 888 nanometers for all experiments. I will show the 3 different temperatures and give a master chart of each of the 3 runs per temperature.

Figure 4.15 shows the 60 ^{o}C kinetic experiment for the first run, it also should be noted that the extinction coefficient ε was calculated to be 112.1 dm^3 mol^{-1} cm^{-1}.

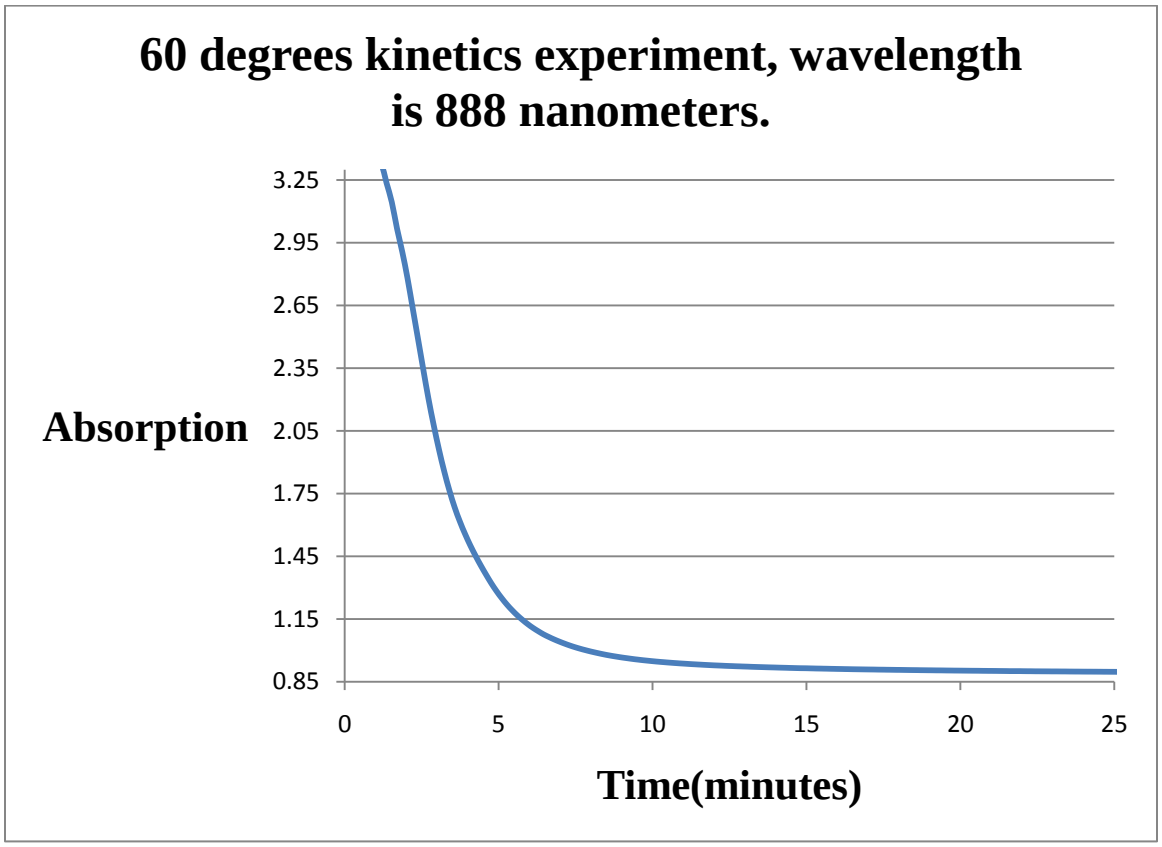

Figure 4.15. 60 ^{o}C kinetics experiment.

Figure 4.16 shows the 70 ^{o}C kinetics experiment showing the first run.

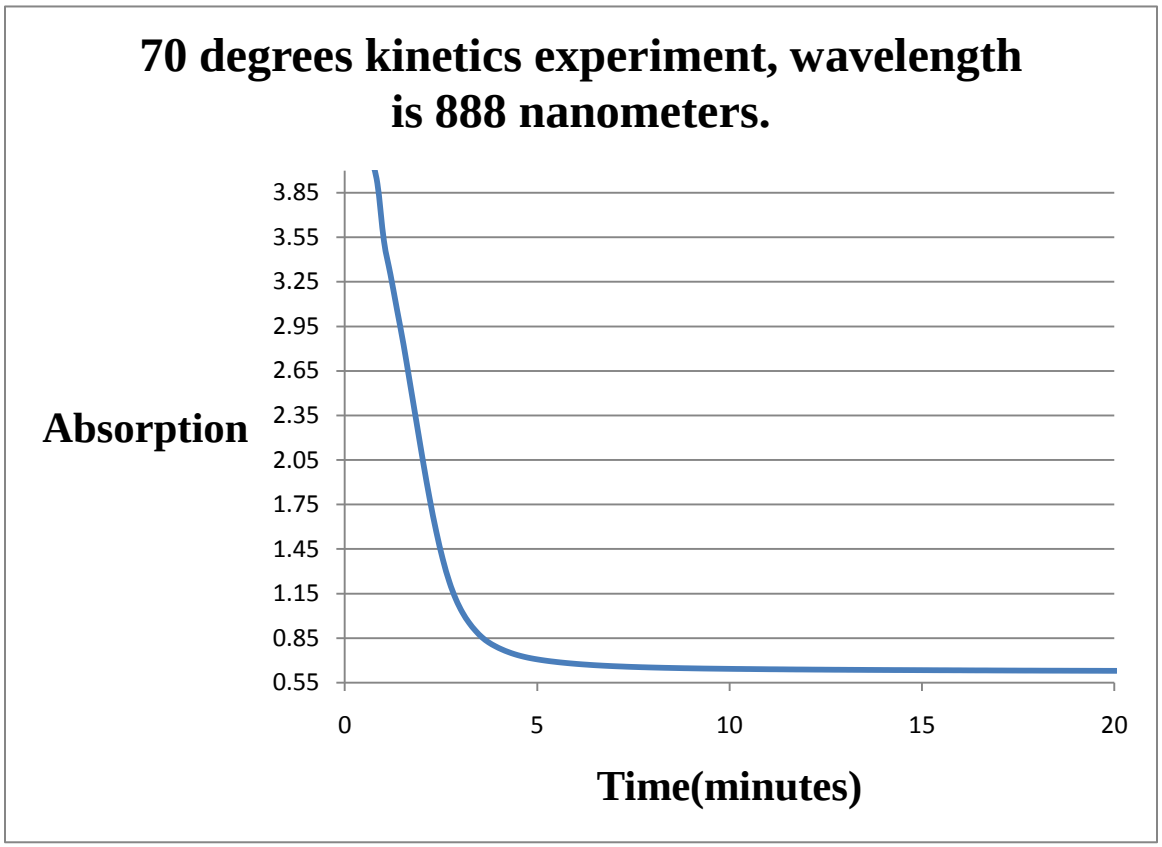

Figure 4.16. 70 ^{o}C kinetics experiment.

Figure 4.17 shows the 80 ^{o}C kinetics experiment showing the first run.

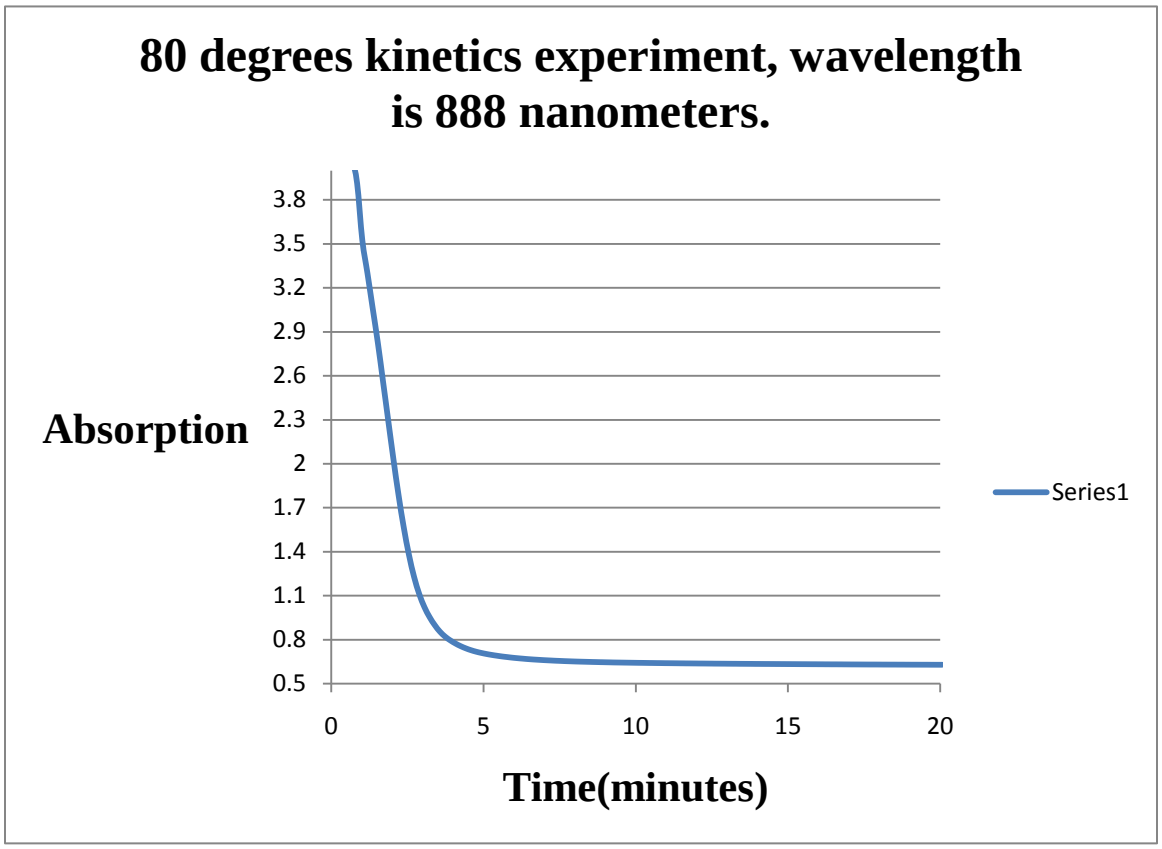

Figure 4.17. 80 ^{o}C kinetics experiment.

What Figures 4.15, 4.16, and 4.17 demonstrate is that as the temperature is raised the dimer complex shown in scheme 4.1 shifts its equilibrium towards the monomer state. To calculate the activation energy plots of ln(concentration) vs time of the above graphs was made. From the plots of the ln(concentration) vs time the slope of each linear plot gave k. "It is found experimentally for many reactions that a plot of ln k against 1/T gives a straight line. This behavior is normally expressed mathematically by introducing two parameters, one representing the intercept and the other the slope of the straight line, and writing the Arrhenius equation ln k= ln$A^{Ea/(RT)"34}$ Table 4.2 will organize the above ideas.

Table 4.2

Arrhenius equation data

^{o}C	$k_{average}$	Kelvin	X equals 10^3 Kelvin divided by T	y equals natural log of k
60	5.1E-03 +/-2.57E-04	333.15	3.0	-5.3
70	9.8E-03 +/-7.1E-04	343.15	2.9	-4.6
80	1.6E-02 +/-1.0E-03	353.15	2.8	-4.1

Figure 4.18 will plot from table 4.2 the lnk vs temperature.

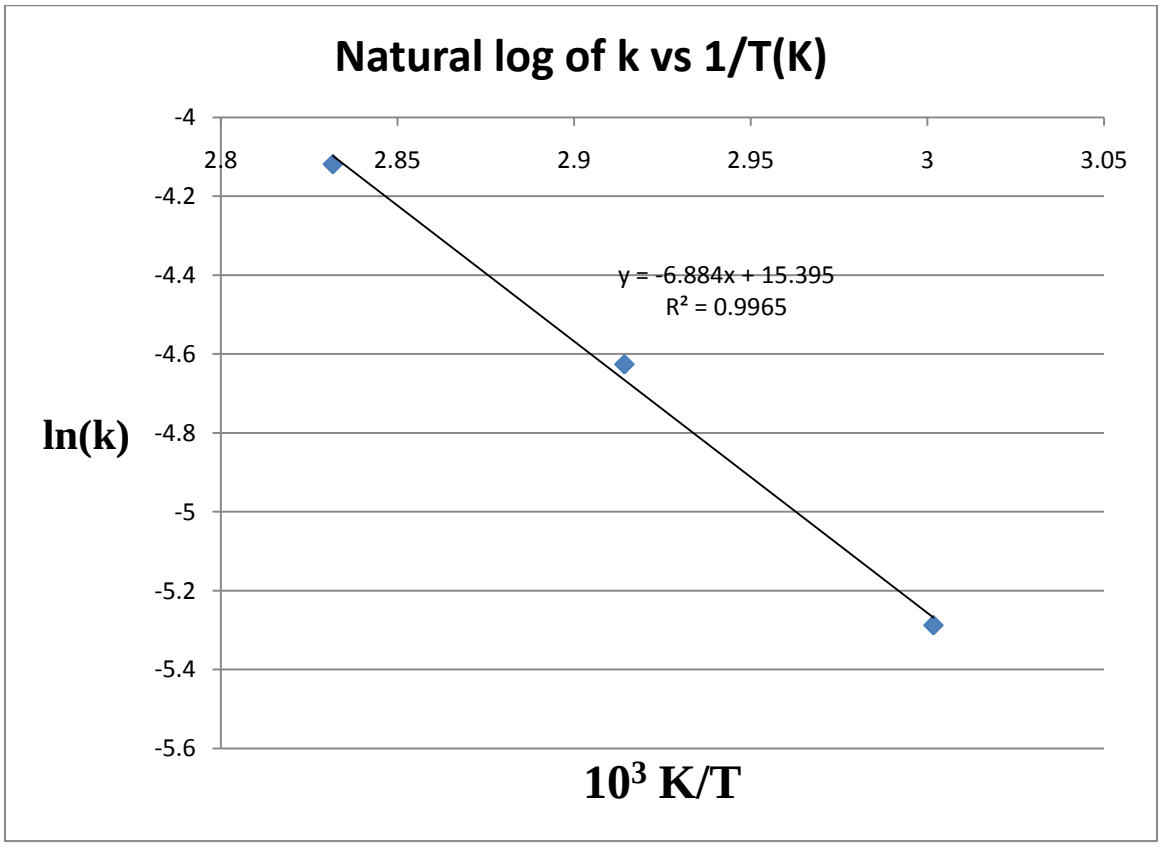

Figure 4.18. Natural log of k versus temperature.

From the slope which is equal to $-E_a/R$ the activation energy can easily be calculated. Ea was found to be 57 kJ mol^{-1}.

Gibbs free energy can be calculated for the above system. There has to be two assumptions when calculating the Gibbs free energy. The first assumption is at the start of the reaction negligible monomer is present. The 2nd assumption is there is a monomer-dimer equilibrium.

Table 4.3 Gibbs free energy information.

Temp in ^oC	Absorption	[Dimer]	[monomer]	$[monomer]^2$	k_{eq}
25	3.5	0.03125	0	0	
60	0.9	0.0080357	0.0232	0.0005389	14.911
70	0.63	0.005625	0.0256	0.00065664	8.566
80	0.46	0.004107	0.0271	0.00073673	5.574

Where the concentration of the [Dimer} is found by dividing by the extinction coefficient. The [monomer] is found by subtracting the [Dimer] at 25 ^oC from the corresponding temperatures, and k_{eq} is found by $[Dimer]/[monomer]^2$.

A plot of ln (K_{eq}^{-1}) vs 1/T is then plotted which is shown in Figure 4.19.

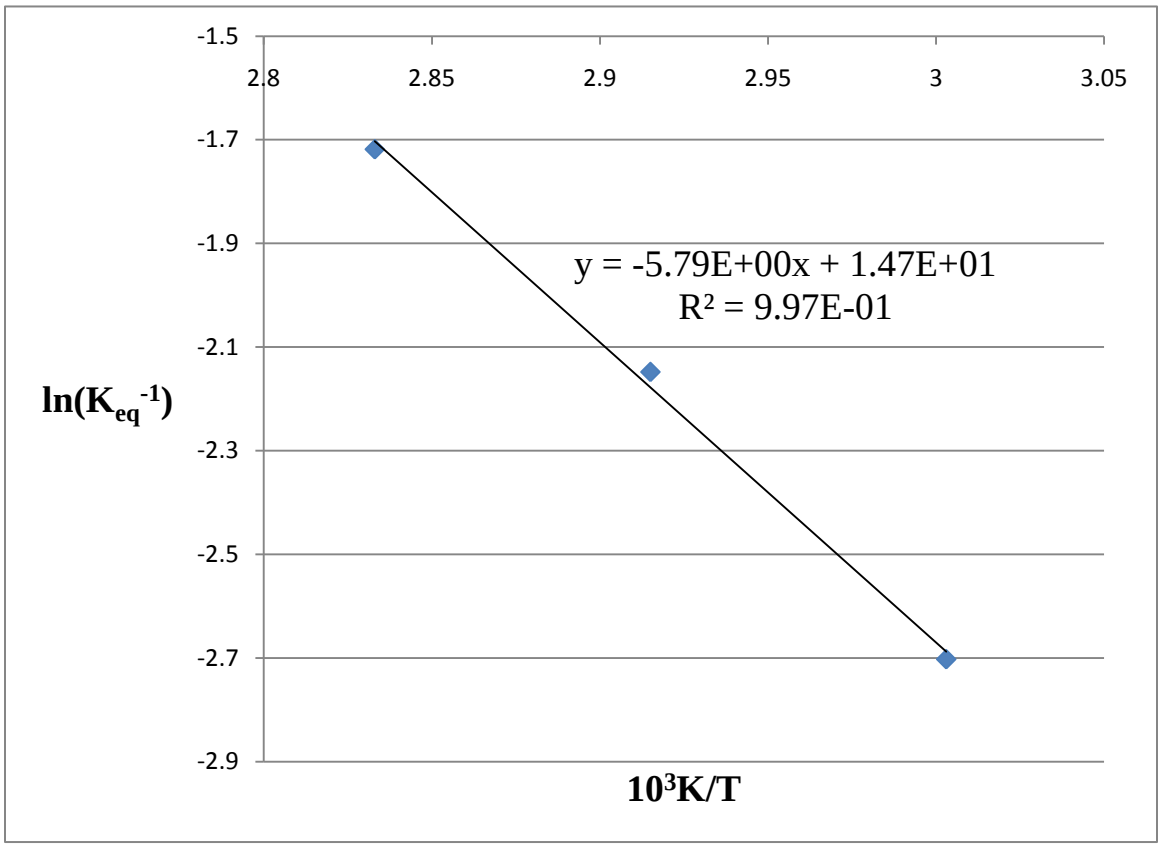

Figure 4.19 Natural log of $1/K_{eq}$ vs temperature^{-1}.

From the slope which corresponds to $\Delta G=-m(R)$, ΔG is found to be 48.8 kJ mol^{-1}, which is experimentally seen where the monomer wants to be in the dimerized form.

Ramos et al. performed a similar experiment where the Ramos group reacted disodium molybdate dehydrates with commercially available D-gluconic acid.[35] Ramos et al. performed several different metal to ligand ratios of the above listed reagents but particular reaction that we were interested in that Ramos did was the 2:1 metal to ligand ratio. The ^{13}C NMR reveals the following placement of the carbon atoms on the gluconate molecule which is demonstrated in figure 4.20.[35]

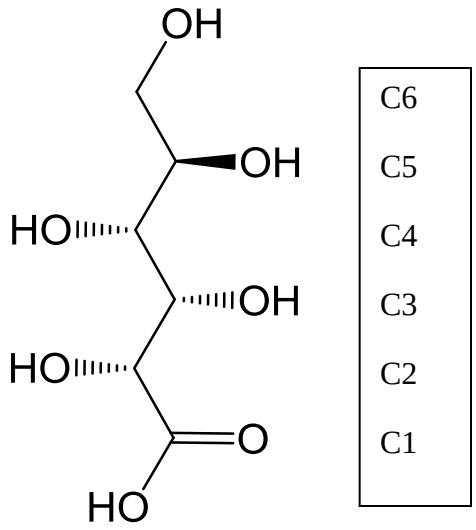

Figure 4.20. Location of carbon in gluconic acid by ^{13}C NMR. [35]

"The available ^{13}C and ^{1}H NMR parameters point to the involvement of O2-O3 and O4 in complexation, besides the carbohydrate group. The complex is probably a tetradentate species possessing the central diol group in an threo configuration, the ligand being in a zig-zag arrangement."[35] The 2:1 metal to ligand ratio of the Ramos paper is shown in Figure 4.21.

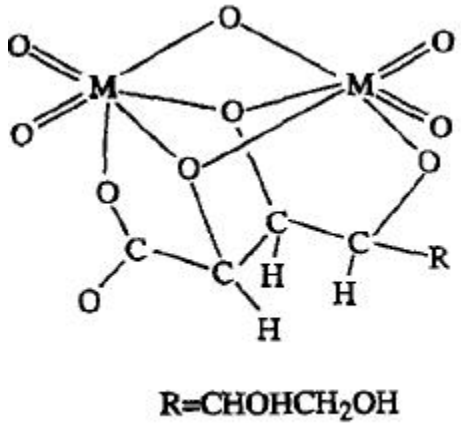

Figure 4.21. Dimerized structure from Ramos paper. [35]

How the ^{13}C of the dimerized form compared to the ^{13}C from the Ramos paper is summarized in Table 4.4. The nuclear magnetic resonance(NMR) apparatus used to take the ^{13}C analysis was a UNITY INOVA 400 NB NMR.

Table 4.4

^{13}C NMR data of blue dimerized compound compared to Ramos paper. [35]

Complex	C-1 ppm	C-2 ppm	C-3 ppm	C-4 ppm	C-5 ppm	C-6 ppm
Ramos paper[35]	184.56	84.35	83.51	82.92	73.37	64.03
Dimerized form	183.256	85.737	83.891	82.822	71.344	63.002

Using infrared spectroscopy there was seen symmetric Mo=O, anti-symmetric Mo=O, COO, and a broad OH peak were all observed. The dimerized material was compared to Fred W. Moore and Richard E. Rice. The Rice group using the compound $MoO_2(CH_3COCHCOC_6H_6)_2$ in KBr observed a symmetric Mo=O stretch at 939 cm^{-1}, and an antisymmetric Mo=O stretch at 909 cm^{-1}.[36] Table 4.5 shows the dimerized form compared with the Rice group data, infrared spectroscopy was gather using a Magna-IR spectrometer 750 Nicolet.

Table 4.5

2.0 Sodium Gluconate 1.0 Molybdenum Trioxide

Group	Compound	Sym Mo=O cm^{-1}	Antisym Mo=O cm^{-1}	COO stretch cm^{-1}
Fred. W. Moore, Richard E. Rice	$MoO_2(CH_3COCHCOC_6H_6)_2$	939	909	
Apblett group	Dimerized blue compound	933	901	1643

All contents of reaction 4.1 went into solution indicating that the two gluconates chelated to the MoO_2^{2+}. Apblett et al. did a similar reaction using gadolinium.[37] Apblett's group took gadolinium carbonate and refluxed that with gluconic acid to make the gadolinium salt. Apblett's group then took the gadolinium salt and reacted it with MoO_3 in a Gd:Mo of 2:3. The structure that Apblett's group is shown in Figure 4.22

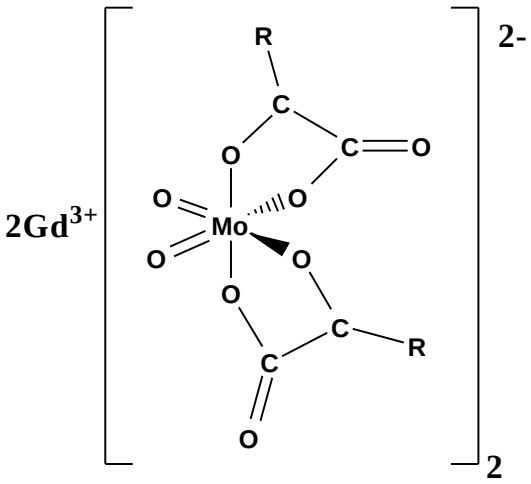

Figure 4.22. Structure of $Gd_2(MoO_4)_3$ Precursor{R= CH(OH)-CH(OH)-CH(OH)-CH_2OH}.[37]

The structure of the sodium salt of the 2.0 equivalents sodium gluconate and 1.0 equivalent MoO_3 is shown in Figure 4.23.

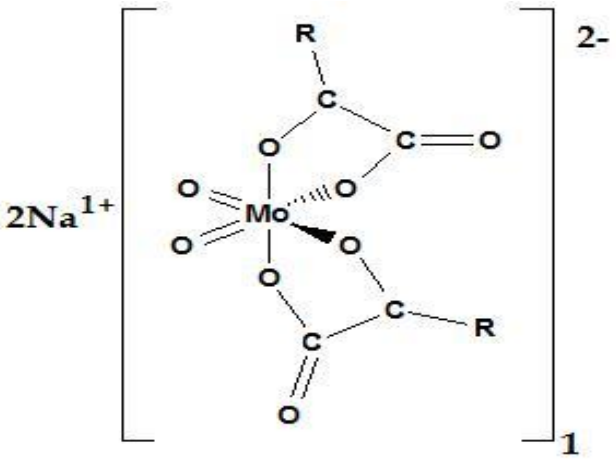

Figure 4.23. 2.0:1.0 sodium gluconate/molybdenyl structure. [35]

The Ramos group[11a] that was previously discussed in chapter four did a similar reaction using a 1:2 (Metal:ligand), the Ramos group came up with the following two diastereomers for the 1:2 (Metal:ligand), which are shown in Figure 4.24. [35]

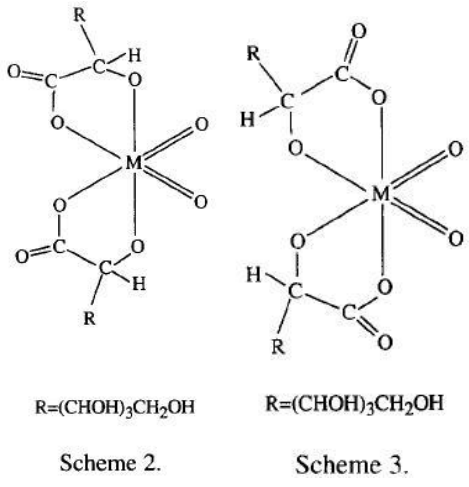

Figure 4.24. Ramos structure of 1:2 (metal:ligand). [35]

Ramos stated the difference between Scheme 2 and 3 in the above Figure 4.24 was Scheme 2 was slightly more stable due to sterics. Scheme 2 is *trans* isomer while Scheme 3 is the *cis* isomer.

Table 4.6 Compares the ^{13}C from the Ramos paper to the ^{13}C from the synthesis of the 2:1 sodium gluconate to molybdenum trioxide complex.

Table 4.6

^{13}C NMR data of 2:1 sodium gluconate to molybdenum trioxide. [35]

^{13}C Spectra	C1	C2	C3	C4	C5	C6
Ramos scheme 2	185.25	86.24	72.55	73.64	73.22	64.12
Ramos scheme 3	184.15	87.98	72.55	73.64	73.22	64.12
Chapter 2:1 Sodium Gluconate to Molybdenum trioxide complex	183.30	87.49	74.22	72.22	71.24	62.79

As can be seen from Table 4.6 there is some slight variation in the position of the carbons in the ^{13}C NMR, but overall the carbons line up with Ramo's diastereomers.

Infra-red spectroscopy was run on the $MoO_2(gluconate)_2$ and was compared to Fred W. Moore, and Richard E. Rice infra-red spectroscopy on a similar structure which was $MoO_2(CH_3COCHCOC_6H_6)_2$.[38] The infra-red spectroscopies of $MoO_2(CH_3COCHCOC_6H_6)_2$ and $MoO_2(gluconate)_2$ are compared in Table 4.7 it should be noted that in the $MoO_2(gluconate)_2$ a broad alcohol peak was observed.

Table 4.7

Raman data of 2:1 sodium gluconate to molybdenum trioxide.[38]

Compound	Symmetric Mo=O cm^{-1}	Antisymmetric Mo=O cm^{-1}	COO stretch cm^{-1}
$MoO_2(CH_3COCHCOC_6H_6)_2$	939	909	
$MoO_2(gluconate)_2$	925	893	1640

Raman spectra confirms Mo=O frequency. O. F. Oyerinde *et al.* did theoretical calculations to investigate possible structures of molybdic acid from raman spectroscopy analysis.[39] O.F. Oyernide *et al.* observed a Mo=O stretching in raman at 919 cm^{-1}. The $MoO_2(gluconate)_2$ complex synthesized in chapter five showed a Mo=O stretching in raman at 921 cm^{-1}.

Conclusions

This project has demonstrated the ability of taking MoO_3 and converting it into a material being nanometric such as was the case of the butanol bronze or a molecular compound which was the case of the dimerized form of MoO_3 with sodium gluconate to effectively make a ink material that is capable of detecting H_2O_2 at concentrations as little as 206 ppm. The blue ink material could also be used in neutralizing explosives.

The project dealing with the sodium gluconate is very promising due to the fact that the solvent of choice is H_2O.

There are many more things to learn and to discover out there with the sodium gluconate and MoO_3 dimerized material. There's many opportunities in future research to try different α-hydroxy acids and to see how well or how well they don't work in detecting H_2O_2. Or to take these materials and see there effectiveness in reducing potential hazardous materials into a viable compound that wouldn't be so dangerous to humans.

I wish everyone the best in future research in this project and to sometimes expect that the unexpected and to be willing to try things even though they might not make sense at the time. Such as when I put a vial of diluted dimerized blue ink in the refrigerator, it first started off as a clear color, but when back into its blue ink. Sometimes science is discovered by accident, and coincidences, so just be willing to try new things and you never know what might happen. Thank you.

References:

1. Meyer, R., *explosives*. Verlag Chemie: New York, 1977; p 358.

2. CNN Judge denies bail to accused shoe bomber. http://archives.cnn.com/2001/US/12/28/inv.reid/ (accessed 9-26-2010).

3. Unstable247 Detailed Description of the Synthesis of Acetone Peroxide. (accessed 9-26-2010) http://cafe.combackalive.com/viewtopic.php?=1&t=20063.

4. Milas, N. A.; Golubovic, A., Studies in Organic Peroxides. XXVI. Organic Peroxides Derived from Acetone and Hydrogen Peroxide. *Journal of the American Chemical Society* **1959,** *81* (24), 6461-6462.

5. Meyer, R. *Explosives*. Weinheim, New York, 1977.

6. Buttigieg, G. A.; Knight, A. K.; Denson, S.; Pommier, C.; Denton, M. B., Characterization of the explosive triacetone triperoxide and detection by ion mobility spectrometry. *Forensic Science International* **2003,** *135*, 53-59.

7. Muller, D; Levy A; Shelef R; Abramovich-Bar S; Sonenfeld D; Tamiri T, *J. Forensic Sci* **2004** *49*, 935-938.

8. Denekamp, C.; Gottlieb, L.; Tamiri T,; Tsoglin, A.; Shilav R.; Kapon, M., Two Separable Conformers of TATP and Analogues Exist at Room Temperature. *Organic Letters* **2005,** *7* (12), 2461-2464.

9. Shakhashiri, B. Z., *Chemical Demonstrations*. 1st ed.; Madison, 1983; p 46.

10. Legler, L., Ueber Producte der langsamen Verbrennung des Aethyläthers. *Berichte der deutschen chemischen Gesellschaft* **1885,** *18* (2), 3343-3351.

11. (a) Ramos, Luisa, Gil, Victor, NMR spectroscopy study of the complexation of D-gluconic acid with tungsten(VI) and molybdenum(VI). *Carboydrate Research* **1997,** *304*, 97-109; (b) Sobkowski, M. HMTD structure. http://en.wikipedia.org/wiki/File:HMTD_structure.png (accessed 10-5-2010).

12. Schaefer, W. P.; Fourkas, J. T.; Tiemann, B. G., <structureofhexamethylenetriperoxidediamine.pdf>. *J. Am. Chem. Soc.* **1985,** *107*, 2461-2463.

13. Davis, T. L., *The Chemistry of Powder and Explosives*. 1st ed.; 1943; Vol. Complete Volume, p 451-453.

14. (a) Wohler, F., *Ann. Chim. Phys* **1825,** *29*; (b) Wohler, F., *Philos. Mag* **1825,** *66*.

15. Greenblatt, M., Molybdenum oxide bronzes with quasi-low-dimensional properties. *Chemical Reviews* **1988,** *88* (1), 31-53.

16. Stavenhagen, A.; Engels, E., *Berichte der deutschen chemischen Gesellschaft* **1895,** *28*, 2281.

17. Wold, A.; Kunnmann, W.; Arnott, R. J.; Ferretti, A., Preparation and properties of Sodium and Potassium Molybdenum Bronze Crystals. *Inorganic chemistry* **1963,** *3*, 545-547.

18. Ehrenfeld, C. H., *Journal of the American Chemical Society* **1895,** *17* (5), 381-397.

19. Dickens, P. G.; Short, A. T.; Crouch-Baker, A., The Crystal Structure of D1.7MoO3 By Powder Neutron Diffraction. *Solid State Ionics* **1988,** *28-30* (1294-1299).

20. Adams, S. http://peggy.uni-mki.gwdg.de/docs/adams/bronzes.html (accessed 10-25-2010).

21. Glemser O; Lutz G, *Z. Anorg. Allg. Chem* **1951,** *264*.

22. Glemser O; Lutz G, *Z. Anorg. Allg. Chem.* **1952,** *269*, 93.

23. Glemser O; Lutz G, *Z. Anorg. Allg. Chem* **1956,** *285*, 173.

24. Birtill, J; Dickens, P, Phase Relationships in the system HxMoO3 ($0<x\leq2.$). *Mat. Res. Bul.* **1978,** *13*, 311-316.

25. West, A. *Solid State Chemistry and its Applications*. John Wiley & sons ltd.: 1984; p 734.

26. Smart, L. E.; Moore, E. A., *Solid State Chemistry*. Third Edition ed.; 2005; p 407.

27. Schulte-Ladbeck, R.; Vogel, M.; Karst, U., Recent method for the determination of peroxide-based explosives. *Anal Bioanal Chem* **2006,** *386*, 559-565.

28. Dubnikova, Faina; Almog, Joeseph; Zeiri, Yehuda; Boese, Roland; Alt,Aaron;Keinan,Ehud; Decomposition of Triacetone triperoxide Is an Entropic Explosion. *J. Am. Chem. Soc* **2005,** *127* (4), 1146-1159.

29. Oxley, J., *In: Schubert H, Kuznetson A (eds) Detection and disposal of improvised devices.* Springer: New York, 2006.

30. Sulzle, D.; Klaeboe, P., The Infrared, Raman and NMR Spectra of Hexamethylene Triperoxide Diamine. *Acta Chem. Scand., Ser. A 42* **1988**, 165-170.

31. Sanchez, J. C.; Trogler, W. C., Polymerization of a boronate-functionalized fluorophore by double transesterification: applications to fluorescence detection of hydrogen peroxide vapor. *Journal of Materials Chemistry* **2008,** *18*, 5129-5133.

32. Hong, J.; Maguhn, J.; Freitag, D.; Kettrup, A., Determination of H_2O_2 and organic peroxides by high-performance liquid chromatography with post-column UV irradiation, derivatization and fluorescence detection. *Fresenius J Anal Chem* **1998,** *361*, 124-128.

33. Determination of Hydrogen Peroxide Concentration (0.1% to 5%). http://www.solvaychemicals.us/static/wma/pdf/6/6/2/5/XX-122.pdf (accessed 11-10-2010).

34. Atkins, Peter; *Atkins' Physical Chemistry*. 8th ed.; 2006.

35. Ramos, Luisa, M. M. C., Gil, Victor; NMR spectroscopy study of the complexation of D-gluconic acid with tungsten(VI) and molybdenum(VI). *Carbohydrate Research* **1997,** *304*, 97-109.

36. Moore, Fred; R. E. R., Physicochemical and Spectral Properties of Octahedral Dioxomolybdenum(VI) complexes. *Inorganic Chemistry* **1968,** *7* (12), 2510-2513.

37. Apblett, Allen; Reinhardt, Larry;, Novel Routes to Ferroelectric Gadolinium Molybdenum Oxides.

38. Moore, Fred; Physicochemical and Spectral Properties of Octahedral Dioxomolybdenum (VI) complexes. *Inorganic Chemistry* **1968,** *7* (12), 2510-2513.

39. Oyerinde, O. R., Solution structure of molybdic acid from Raman spectroscopy and DFT anaylsis. *Inorganica Chimica Acta* **2008,** *361*, 1000-1007.

VITA

Derek Davin Bussan

Candidate for the Degree of

Master of Science

Thesis: CHEMISTRY OF HYDROGEN MOLYBDENUM BRONZES AS A SENSOR DEVICE

Major Field: CHEMISTRY

Biographical:

Personal Data:

Born in Dubuque Iowa, on July 7th, 1982, son of Ronald and Michelle Bussan.

Education:

Completed the requirements for the Master of Science in Chemistry At Oklahoma State University, Stillwater, Oklahoma in May 2011.Completed the requirements for the Bachelor of Arts in Chemistry at University of Iowa, Iowa City, Iowa in 2004.

Experience:

Employed as a teaching assistant by Oklahoma State University, Department of Chemistry, 2008-2009, and then from 2010-2011. Employed As a research assistant by Oklahoma State University Department of Chemistry, 2009-2010.

Professional Memberships:

Phi-Lambda-Upsilon (PLU) professional chemistry honor society.

Name: Derek Bussan Date of Degree: May, 2011

Institution: Oklahoma State University Location: Stillwater, Oklahoma

Title of Study: APPLICATIONS OF MOLYBDENUM UTILIZED IN SENSING DEVICES

Pages in Study: 71 Candidate for the Degree of Master of Science

Major Field: Chemistry

Scope and Method of Study: Peroxide-based explosives such as TATP and HMTD have been used in numerous terrorist attacks worldwide and, even in Oklahoma, people have been injured and killed by these dangerous explosives. There have also been attempts to smuggle ingredients for peroxide-based explosives onto aircraft to produce bombs during flights.

Findings and Conclusions: A cost effective, and quick method for detecting peroxide based explosives was developed that utilizes the dramatic color change from blue to white when Mo(V) centers in molybdenum bronzes react with peroxides. In this thesis two mechanisms are discussed by which this process takes place. One which utilizes molybdenum trioxide with butanol as the solvent. The 2nd method in this thesis is a reduction of molybdenum trioxide by aqueous sodium gluconate in a one-pot synthesis of a dark blue ink that is sensitive to H_2O_2. This ink can be used to produce test strips that can detect H_2O_2 at concentrations as little as 206 ppm, well below the concentration that it would actually take to make an effective explosive.

ADVISER'S APPROVAL: Dr. Allen Wallace Apblett